quantum reports

IMPACT FACTOR 1.3

CITESCORE 3.0

Article

The Periodic Table as an Emergent Helicoidal Manifold: A Unified Information-Theoretic Analysis of the Atomic Elements $Z = 1–103$

Rodolfo O. Esquivel, Hazel Vázquez-Hernández and Jonathan Ornelas-Muñoz

MDPI

https://doi.org/10.3390/quantum8010022

quantum reports

MDPI

Article

The Periodic Table as an Emergent Helicoidal Manifold: A Unified Information-Theoretic Analysis of the Atomic Elements $Z = 1$–103

Rodolfo O. Esquivel [1,2,*], Hazel Vázquez-Hernández [1] and Jonathan Ornelas-Muñoz [1]

[1] Departamento de Química, Universidad Autónoma Metropolitana, Mexico City 09340, Mexico
[2] Instituto Carlos I de Física Teórica y Computacional, Universidad de Granada, 18071 Granada, Spain
* Correspondence: esquivel@xanum.uam.mx

Abstract

Here we perform a detailed information-theoretic (IT) analysis of atomic electron densities in the periodic table, from hydrogen (Z = 1) to lawrencium (Z = 103). By use of the Shannon entropy, the Fisher information and the disequilibrium functionals in both position and momentum spaces as fundamental descriptors of the atomic densities, the periodic table can be represented in a three-dimensional information space as a continuous, highly ordered manifold. The analysis shows that chemical periodicity naturally emerges as a helicoidal manifold (reminiscent of a helix) at the coordinates of a 3D theoretic-information space (Shannon, Fisher, Disequilibrium), with each period forming one segment within the continuous global trajectory. We find information-theoretic signatures of shell structure, sub-shell filling, and electron-configuration anomalies, such as the familiar irregularities seen in chromium and copper. Therefore, the helicoidal character emerges naturally and is not imposed a priori. Further, through the uncertainty principle of the complementary analysis in momentum space, more insights are gained by exposing maximal information-theoretic differentiation for lighter atoms and compression among heavy elements. Notably, momentum-space analysis reveals that hydrogen occupies a natural intermediate position between helium and lithium based on kinetic energy distribution—contrasting with IT position-space results that emphasize hydrogen's unique delocalized electron density. Indeed, the 3D IT representation of the elements in position space aligns with the view that H does not belong to either the alkali metals or the halogens, but rather stands as a unique, standalone element. This complementary perspective provides new quantitative support for understanding hydrogen's dual chemical nature, providing new quantitative insight into ongoing debates about hydrogen's optimal periodic table position. Furthermore, by considering triadic relationships and complexity properties in relation to the López–Mancini–Ruiz (LMC) and Fisher–Shannon (FS) functionals, we show that atomic complexity increases monotonically along with nuclear charge, and we provide a quantitative measure of how organized atomic electron densities are distributed throughout the periodic system. Based on our IT analyses, the fundamental character of periodicity could be addressed by employing helicoidal representations that highlight the characteristics of hydrogen, while simultaneously preserving the autonomy of the blocks of elements.

Keywords: periodic table; information theory; Shannon entropy; Fisher information; complexity measures; periodic helical representation; elements classification

Academic Editor: Gerald B. Cleaver

Received: 30 November 2025
Revised: 24 February 2026
Accepted: 7 March 2026
Published: 12 March 2026

1. Introduction

The periodic table of chemical elements stands as one of the most profound achievements in the history of science, representing not merely a classification scheme but a fundamental expression of natural laws [1,2]. Since 1869, when Dmitri Mendeleev's groundbreaking work laid the foundation for basic chemical behavior, the periodic system has developed from a mechanism for grouping known elements into a predictive framework that continues to inform chemical research and understanding [3,4]. Almost 150 years later, despite efforts of nearly 150 years of many chemists and physicists who have contributed in exploring these concepts, fundamental questions concerning the optimal representation and grouping of elements—most prominently concerning hydrogen and helium—are still discussed [5,6].

1.1. Historical Development and Continuing Problems

An early insight into this dynamic evolution was demonstrated by Mendeleev's 1869 original periodic table, which placed hydrogen in a position disconnected from other elements and their characteristics, reflecting even at that early stage an awareness of its unique chemical behavior [1]. In his table from 1871, hydrogen was listed at the head position of the alkali metals in Group I, and this rank continued to hold a prominent position in most modern tables [2,5]. This was enabled by hydrogen's lone valence electron and ability to form unipositive ions, properties typical of the alkali metals. Nevertheless, this categorization has never been entirely precise, because hydrogen also exhibits characteristics that allow it to be identified in a way comparable to the halogens (diatomic molecules, stable anions) [7–9]. Similar issues arise with helium. Despite being placed among the noble gases in the standard periodic table because of its chemical inertness and fully occupied valence shell, helium's electronic configuration ($1s^2$) is exactly like that of the valence shells of alkaline earth metals [10,11]. Others have suggested alternative positions, particularly in Charles Janet's left-step periodic table, where helium is represented at the head of the alkaline earth metals [12–14]. The challenge of definitively qualifying either of these elements speaks to a broader epistemological inquiry: what is the most basic criterion for the classification of elements? Various attempts have been made by the periodic system to address such problems, stemming from Mendeleev's original work based on atomic masses and chemical properties to contemporary quantum mechanical descriptions of the periodic system based on electronic configurations [15,16]. Each approach offers insights, yet none has succeeded in resolving all the anomalies and ambiguities within the system [4,5].

1.2. Criteria for Element Classification

Contemporary approaches to organizing the periodic table typically invoke several distinct criteria, each with its own strengths and limitations. Nowadays, the quantum mechanical approach, based on electronic configurations and the number of valence electrons, has become dominant in modern chemistry education [11,17]. It is this basis for scientific theory that accounts for a large part of the periodicity that underlies the chemical system. Nevertheless, as Scerri stressed, the possession of a particular number of outer-shell electrons is "neither a necessary nor a sufficient condition for an element's being in any particular group" [4]. Notable exceptions include transition-metal triads such as nickel–palladium–platinum, which do not share identical valence configurations yet clearly belong to the same group based on chemical behavior [16,18].

Electronegativity has been proposed as an alternative classificatory principle, with proponents arguing that this property better captures chemical similarities and reactivity patterns [19–21]. Sanderson's rational periodic table placed hydrogen at an intermediate position between boron and carbon based on electronegativity values, while others

have used this criterion to position hydrogen between alkali metals and halogens [19,22]. However, the existence of multiple electronegativity scales and ongoing debates about the fundamental nature of this concept complicate its use as a primary organizational principle [21].

A third approach, recently revived by Scerri, employs the concept of triads—sets of three elements whose atomic numbers form arithmetic progressions [23,24]. This criterion, originally proposed by Döbereiner in terms of atomic weights, becomes exact when reformulated using atomic numbers. According to this perspective, hydrogen should be placed among the halogens, forming the triad H(1)-F(9)-Cl(17), while helium correctly heads the noble gases in the triad He(2)-Ne(10)-Ar(18) [23]. This approach has the appeal of mathematical precision but has been questioned regarding its physical basis and explanatory power [18,25].

1.3. Anomalies and Alternatives

In addition to the hydrogen–helium placement problem, the periodic system is riddled with other familiar anomalies that do not lend themselves to simple organizational schemes. Three pairs of elements exhibit inversions in the atomic mass sequence relative to atomic number, argon–potassium, cobalt–nickel, and tellurium–iodine [26]. These anomalies have straightforward explanations rooted in isotopic abundance and nuclear stability. The argon–potassium inversion followed Earth's early loss of primordial argon-36 and subsequent gathering up argon-40 from radioactive decay of potassium-40 [26]. The cobalt–nickel and tellurium–iodine inversions represent the greater nuclear stability of even atomic number elements compared to odd atomic number elements [26].

The question of optimal representation extends beyond element placement to the fundamental format of the periodic system itself. While Mendeleev conceived of the system as fundamentally continuous, noting that "the series of elements is uninterrupted, and corresponds, to a certain degree, to a spiral function" [27], he and the majority of its successors implemented tabular modes, given practical reason [28]. But, tables require artificial breaks in the sequence and may obscure continuity [12,28]. In the periodic system and throughout its history, various spiral and helical representations have been suggested, from the cylindrical helix by de Chancourtois (1862) down to the current designs [3,28]. These alternative formats also have certain advantages, such as the natural correspondence between periods and true circularity, as well as the avoidance of arbitrary row divisions [13,28–30].

1.4. Central Positioning and Spiral Representations

A groundbreaking solution to the hydrogen placement problem was suggested by Kaesz and Atkins [31], who proposed a position in which hydrogen would be placed at the center and head of the periodic table, neither in Group 1 nor Group 17, but rather within the position of the unique character of the matter [31]. This placement allows us to understand that hydrogen is different from both alkali metals and halogens in many ways: it creates H^- anions (in contrast to alkali metals) and can be expressed as diatomic H_2 compounds (like halogens), but it has limited typical metallic or halogenic features. According to this view, the arrangement of hydrogen with arrows indicating its relationships to both alkali metals and halogens better corresponds to its dual chemical nature without forcing it into either group [31].

Spiral representations of the periodic system have extended this idea of central positioning. A novel square spiral configuration was proposed by Rodríguez Peña and García Guerra, who suggest that hydrogen is normally located in the center of the periodic system, from which the table unfolds outward in a counter-clockwise direction [32]. The hydrogen

is on top of the lithium in this configuration but passes over fluorine to reach helium in this configuration, a way of visually presenting that hydrogen is a dual type of alkali–halogen while preserving the periodic sequence. This spiraled arrangement avoids spurious cuts between noble gases and alkali metals by reading natural and identifying blocks of the orbit with protrusions free of disruption [32].

The concept of spiral representations as fundamental to understanding periodicity has been introduced by Imyanitov, where the spiral form is proposed as the simplest description of periodicity and transitions from a simple to complex form [33]. Simply having nuclear charge arranged by the linear sequence of elements, in a spiral, is a very good representation that can then be transformed by compression, bending, and cutting into other formations, including the table. Imyanitov says that the spiral representation shows that each block of elements is independent, i.e., blocks s, p, d, and f are all different in their shape, height and the number of elements they contain, as well as in the variation of electron shell parameters [33].

Historical precedents for spiral representations date back to Chancourtois's telluric screw (1862) and include various models documented by Scherer, who cataloged a few and described which types of spiral periodic charts were best for the chemical relationships [34]. An example of such an early spiral model of the periodic system was the model by Charles Janet in the mid-20th century [35]; his principles became the foundation for the left-step periodic table, which organizes the elements by orbital filling order, giving helium to the alkaline earth metals [12,13,36]. Although such placement of helium is controversial from a chemical perspective, the left-step has been reappraised for its mathematical polish and for matching with the $(n + \ell)$ rule (Madelung rule) for orbital filling [14,25,37]. Even more unexpectedly, Janet predicted all of the major scientific advances with his theoretical work on atomic structure. However, even though he worked up until the discovery of the neutron, he rightly predicted the existence of deuterium (heavy hydrogen), helium-3, and what we now call neutronium (element zero, with dineutrons) [35,36]. His speculation that neutronium could be an intermediate between matter and antimatter was particularly prescient, predating Dirac's theoretical study for antimatter [35,36]. Janet predicted the identification of transuranium elements and implicitly assumed a $(n + \ell)$ rule 6 years before Madelung found it [35,36].

An equally impressive but largely overlooked contribution to the development of the periodic system representations comes from the Russian physicist Viatscheslaw Romanoff, who had the foresight to introduce, as early as 1934, fundamental concepts that would not become widely recognized for another forty years [38]. Romanoff's periodic table effectively brought together the approaches of Werner—or, in this case, Janet—to form something that can be called "a spiral periodic system on a plane." Romanoff is perhaps best known for being the first to introduce the actinide series, a decade prior to Glenn T. Seaborg presents the actinide theory through his famous 1944 work [38].

1.5. Contemporary Perspectives

Recent attention has highlighted that the difficulty associated with hydrogen and helium is indicative of true complexity rather than accidental bad fortune in history or lack of complete knowledge. In their extensive examination Petruševski and Cvetković state that "depending on the arguments offered, various choices may appear to seemingly lead to the 'best possible choice,' and people are usually biased/predetermined to one of the possible choices" [5]. Their comprehensive study of five positioning strategies for hydrogen—as a member of group 1, group 17, and group 14, as higher than both lithium and fluorine, or as a standalone element—reveals that, as shown in Petrusevski 2018, each has inherent merit with respect to these emphasized criteria [5].

In particular, hydrogen is not merely just hydrogen for chemistry, its nature distinguishes it from the rest of the elements because it can produce H^+ and H^- ions, participates in hydrogen bonding (also a feature unique to hydrogen in such a way that bond strength can vary continuously from van der Waals to covalent bonds), and has stretching frequencies from 3700 to 500 cm^{-1} [5]. The exceptional nature supports Kaesz and Atkins' recommendations for a standalone location in the center, recognizing that hydrogen "lies at the head of the entire table and as such can be expected to be strikingly different from all the elements" [5,31].

Block autonomy offers a different view toward the problems of element classification. An analysis of this phenomenon by Imyanitov shows that the properties of the s, p, d and f blocks behave in fundamentally different ways, although typical in some of the blocks, other blocks exhibit no similar regularities [33]. This autonomy is observable in block widths (2, 6, 10, 14 elements), the placement of differentiating electrons (outer shells versus inner shells) and different profiles of variation in properties across blocks. The existence of block autonomy raises the question that attempts to impose uniform classificatory criteria on all elements are fundamentally misguided [33].

Some have proposed that hydrogen (and maybe helium) be duplicated in the periodic table, appearing in more than one location at once [39,40]. In a similar vein, Atkins and Kaesz proposed the floating position of hydrogen on the top of the main table to represent its peculiar nature while avoiding pushing hydrogen to any given group [31]. But the two approaches have been criticized as violating an underlying "one-element-one-place" principle that has framed periodic table design since Mendeleev [41].

Labarca and Srivaths take a more integrative approach, saying that the three principal classificatory criteria—electronic configuration, electronegativity and atomic number triads—should receive equal epistemological status, rather than privileging any single criterion [6]. In their periodic table, hydrogen lies between alkali metals and halogens and helium lies between noble gases and alkaline earth metals, visually representing this "democratic" relationships between criteria [6]. In this way, the continuity and connectivity of the periodic system are maintained while recognizing its complexity.

The spiral representations discussed earlier offer yet another resolution. By placing hydrogen at the center of a spiral that expands outward through the elements, these formats acknowledge hydrogen's unique status while maintaining the continuity of atomic number progression [32,33]. The spiral format naturally accommodates the changing period lengths (2, 8, 8, 18, 18, 32, 32 elements) with no artificial breaks, and the transition from single element electronic structures to complexity can be visually illustrated in terms of progression or evolution [32,33].

1.6. Information Theory

Alongside the developments in atomic modeling described above, information theory has established itself as a powerful complementary approach for characterizing atomic and molecular structure, chemical bonding, and reactivity patterns. From this viewpoint, Shannon entropy, Fisher information, disequilibrium, and statistical complexity measures offer a mathematically rigorous framework for describing order, dispersion, and internal correlations—derived directly from electronic probability distributions without dependence on basis set selection. These information-theoretic tools have proven particularly valuable for identifying electron delocalization patterns, revealing correlation and localization features, and building quantitative bridges between electronic structure and experimentally observed chemical behavior.

Applying information-theoretic measures to chemical systems has uncovered fundamental connections between electronic structure and molecular properties. Information

planes constructed from entropy and disequilibrium enable differentiation among molecular geometries, bonding patterns, and polarity characteristics, while complexity measures trace the progressive structural enrichment from simple diatomic molecules to biologically relevant amino acids [42,43]. Extensions into momentum space and three-dimensional information density representations provide distinctive fingerprints of equilibrium geometries and enable the tracking of bond dissociation and formation along reaction pathways [44]. Profiles of Fisher information and entropy-based indicators illuminate the localization–delocalization transitions characteristic of transition states, offering a phenomenological description that parallels—though is not directly equivalent to—potential energy barriers [45]. Studies of proton-transfer equilibria in citric acid demonstrate that this framework can address both kinetic and thermodynamic dimensions of chemical reactivity [46].

The scope of information-theoretic analysis further encompasses molecular classification approaches. The Predominant Information-Quality Scheme (PIQS), for instance, evaluates six global descriptors for each molecule—including position- and momentum-space entropies, Fisher information values, and Onicescu disequilibria—assigning a single-letter classification based on the descriptor with the highest normalized value, effectively discriminating among aliphatic, aromatic, polar, and charged amino acid families [47].

Recent advances have broadened the applicability of information-theoretic methods considerably. Shannon entropy, Fisher information, and disequilibrium serve as information-theoretic functionals that characterize probability distributions independently of specific physical parameters. Crucially, these three measures capture fundamentally distinct aspects of electron density and cannot be reduced to simple density integrals. Shannon entropy, employing logarithmic weighting, is particularly sensitive to diffuse, low-density regions and serves as a measure of global delocalization. Fisher information, constructed from density gradients, responds strongly to local density variations and sharp distributional features. Disequilibrium, through its quadratic weighting, emphasizes high-density regions and quantifies deviation from uniformity. Importantly, these measures are interconnected through fundamental information-theoretic inequalities, notably the Cramér–Rao bound and entropy–power relations. The atomic trajectory traced through three-dimensional (S, I, D) space is governed by these constraints, and the resulting helicoidal geometry encodes physical information about electronic organization that remains inaccessible to any single measure in isolation.

It is worth emphasizing that information-theoretic analysis provides objective, quantitative descriptors derived from quantum mechanical calculations without presupposing any particular periodic table format. As we demonstrate in the present work, the helicoidal structure emerges naturally from the IT measures; it is not an assumption of our methodology. In this sense, our results describe a mathematical structure inherent in atomic electronic organization, which can inform—but does not resolve—ongoing discussions about optimal periodic table representations.

1.7. Scope and Objectives

The periodic table of elements is one of the most basic organizing principles of chemistry and physics, encoding systematically how atomic properties change as they become charged with nuclear matter. Traditional methodologies for understanding periodicity rely on quantum mechanical descriptions of electron configurations and orbital filling; information theory provides its own complementary yet alternative, more general framework that expresses these structural features into universal measurements with less dimensions.

Throughout our study we present a unified information-theoretic analysis of the Periodic Table ranging from hydrogen to lawrencium (Z = 1–103) and taking measures in both position and momentum spaces. We find that the periodicity of elements materializes

automatically as a geometrical form (helicoidal trajectory for instance) if atomic electron densities are mapped to the 3D space characterized by Shannon entropy, Fisher information, and disequilibrium. Such a representation not only demonstrates the recognized properties of periodicity but also offers quantitative information on shell geometry, sub-shell filling, and the subtle electronic signatures of chemical anomalies. In the historical description of the periodic system there have been a large variety of 2D spiral models. However, our results indicate throughout this work that a more precise mathematical description corresponds to a helicoidal shape when viewed in three-dimensional information-theoretic space, as opposed to a simple 2D spiral.

It is important to delineate the scope of our analysis. Chemistry under ordinary conditions primarily involves valence electrons, with core electrons remaining essentially inert at typical energy scales (a few eV). Our study characterizes the intrinsic information-theoretic structure of free atoms as the fundamental building blocks of the periodic system, providing a reference framework from which chemical perturbations can be understood. The periodic table itself is organized by total ground-state configurations, and our IT analysis aligns with this organizational principle. A valence-focused information-theoretic analysis would more directly address chemical reactivity and represents a complementary perspective for future investigation.

Several methodological considerations merit acknowledgment. First, the electron density $\rho(\mathbf{r})$ does not retain orbital phase information, which is relevant to chemical bonding. Our analysis intentionally focuses on density-based descriptors because the periodic classification itself is determined by ground-state electronic structure, which is fully encoded in the density. Second, as atomic number increases, the total density becomes increasingly dominated by core electrons, potentially diminishing sensitivity to valence-shell features. Nevertheless, our analysis successfully detects chemically significant anomalies (Cr, Cu, Si), demonstrating that IT measures retain sensitivity to valence-related effects. A complementary analysis focusing exclusively on valence densities could provide additional insights and represents a promising direction for future work.

The paper is structured as follows: Section 2 describes the conceptual foundation of our approach along with the computational method employed to calculate the atomic densities. In Section 3, we present the theoretical framework of information-theoretic measures used in the current study, such as Shannon entropy, Fisher information, disequilibrium, the LMC and Fisher–Shannon complexity functionals. Data statistics are used in Section 4 to validate found correlations on Wilks' Lambda and Random Forest models. The information-theoretical analyses over the periodic table are presented in Section 5 (Z = 1–103), and at the end of Section 6, we summarize our main findings and discuss the potential implications of information-theoretic representations for chemical periodicity.

2. The Periodic Table and the Independent-Particle Model

Prior to discussion of the details of the computational methodology, we would like to clarify the conceptual foundations of our approach. We argue that Hartree–Fock (HF) theory is not merely an acceptable approximation for this study, but is in fact the conceptually appropriate level of theory for an information-theoretic characterization of the periodic table.

The periodic table, as constructed through the aufbau principle, is fundamentally an independent-particle model. Its organizational principles—the Pauli exclusion principle, Hund's rules, and the aufbau sequence—only acquire meaning within a mean-field framework where one can meaningfully speak of "orbitals" and "electron configurations." The very notion of assigning a configuration such as [Ar] $3d^5 4s^1$ to chromium presupposes an independent-particle picture in which electrons occupy well-defined single-particle states.

From the perspective of quantum information theory [48] and density matrix formalism [49], this has important implications:

- The Hartree–Fock method produces a single Slater determinant, representing a pure N-electron state with the density matrix $\hat{\rho} = |\Psi_{\mathrm{HF}}\rangle\langle\Psi_{\mathrm{HF}}|$ satisfying $\mathrm{Tr}(\hat{\rho}^2) = 1$.
- The one-electron reduced density matrix derived from HF is idempotent ($\gamma^2 = \gamma$ for closed-shell systems), consistent with a pure-state description at the single-particle level.
- The periodic table does not encode non-local quantum correlations or entanglement—it is a classification scheme based on mean-field electronic structure. Mixed states, which would require post-Hartree–Fock treatments, are not part of the conceptual framework underlying the periodic system.

In essence, the periodic table addresses an inherently single-particle question: How do electrons sequentially fill orbitals as nuclear charge increases? This is precisely what Hartree–Fock theory is designed to describe.

2.1. Conceptual Alignment Between HF and the Periodic Table

Table 1 summarizes the correspondence between the periodic table's conceptual framework and the Hartree–Fock description:

Table 1. Conceptual correspondence between the periodic table model and Hartree–Fock theory.

Aspect	Periodic Table Model	HF Description
Electronic structure	Independent-particle configurations	Single Slater determinant
Quantum state nature	Pure state	Pure state
Electron density	Superposition of orbital densities	$\rho(\mathbf{r}) = \sum_i \lvert\phi_i(\mathbf{r})\rvert^2$
Origin of periodicity	Shell and sub-shell structure	Captured exactly
Classification basis	Orbital occupations (n, ℓ, m_ℓ, m_s)	Natural framework

2.2. Accuracy of HF Densities for Information-Theoretic Measures

The information-theoretic functionals employed in this work—Shannon entropy $S[\rho]$, Fisher information $I[\rho]$, and disequilibrium $D[\rho]$—are all functionals of the one-electron density $\rho(\mathbf{r})$.

For ground-state atoms, Hartree–Fock densities are remarkably accurate. From perturbation theory, the HF density is identical to the exact density to first order in the correlation perturbation [50], implying deviations are typically within 1–2% of correlated or experimental electron densities [50,51]. This accuracy stems from several factors: (i) The electron density is dominated by core electrons, which are excellently described at the HF level [50], (ii) exchange interactions are included exactly within HF theory, (iii) the spherical symmetry of atomic systems is rigorously preserved, and (iv) while correlation effects are important for precise energetics, they produce only minor perturbations to the overall density distribution [52].

Notwithstanding the above, we acknowledge that electron correlation and relativistic effects are essential for quantitatively accurate predictions of many atomic properties. However, their omission does not compromise the validity of our information-theoretic analysis for the following reasons: correlation energy typically constitutes approximately 1% of the total electronic energy. While this contribution is crucial for chemical accuracy in thermochemical predictions, it does not fundamentally alter shell structure or the periodic organization of elements. Indeed, the periodic table was fully established and understood decades before electron correlation was rigorously formulated. The qualitative features we characterize—shell filling, block structure, and periodic trends—are mean-field phenomena

that exist independently of correlation effects. On the other hand, for heavy elements ($Z > 50$), relativistic effects cause orbital contraction and expansion, as well as spin–orbit splitting. These effects modify quantitative properties but preserve the qualitative periodic structure. The organization of the periodic table into s, p, d, and f blocks remains intact, and the helicoidal structure we identify in information-theoretic space persists throughout the entire range $Z = 1$–103.

Also, it is noteworthy, as we discuss below, that our information-theoretic analysis successfully detects the well-known chemical anomalies associated with chromium ($3d^5 4s^1$), copper ($3d^{10} 4s^1$), and silicon, among others. This demonstrates that the HF description captures the essential physics underlying these deviations, while the IT measures possess sufficient sensitivity to identify subtle configuration effects within the mean-field framework.

Finally we would like to note that for a theoretical model to be consistent, the level of theory should be appropriate to the phenomenon under investigation. Our objective is to characterize the information-theoretic structure of the periodic classification itself—not to predict ionization potentials, electron affinities, or other properties requiring chemical accuracy. The periodic table is, at its core, a mean-field construct. Employing post-Hartree–Fock methods would introduce a conceptual inconsistency: we would be using a theory that goes beyond the independent-particle approximation to study a classification system that is defined within that approximation. The use of Hartree–Fock wave functions ensures that our information-theoretic analysis operates at the same conceptual level as the periodic system itself.

2.3. Computational Methodology

The electronic structure calculations in this work employ Hartree–Fock wave functions as described in [53–55], which provides high-quality analytical representations of atomic orbitals in Slater-type basis sets for elements $Z = 1$–103, in the absence of external fields. The one-particle density in position space, $\rho(\mathbf{r})$, is constructed from the occupied orbitals, and the corresponding momentum-space density $\gamma(\mathbf{p})$ is obtained via three-dimensional Fourier transformation. These one-particle densities ensure methodological consistency with the conceptual framework of the periodic table itself, as discussed in the previous section. However, it is important to remark that the choice of non-relativistic Hartree–Fock theory merits its own discussion, as we presented in Section 2. The periodic table, constructed via the aufbau principle, Pauli exclusion, and Hund's rules, is fundamentally an independent-particle model. The assignment of electron configurations presupposes a mean-field framework in which electrons occupy well-defined single-particle states. Since our objective is to characterize the information-theoretic structure of this classification system—rather than to predict properties requiring post-Hartree–Fock accuracy—the use of HF wave functions ensures methodological consistency with the conceptual framework of the periodic table itself.

3. Information-Theoretic Information Measures

Independent-particle electron densities can be represented in either position ($\vec{r}$-space) or momentum ($\vec{p}$-space). These two complementary representations capture distinct yet related aspects of electronic structure and can shed new light on the nature of atomic periodicity.

3.1. Electronic Density Models

The one-particle electron density in position space, $\rho(\vec{r})$, is constructed by use of the Hartree–Fock orbitals $\psi_i(\vec{r})$ according to the following:

$$\rho(\vec{r}) = \sum_{i=1}^{N} |\psi_i(\vec{r})|^2 \tag{1}$$

where the summation is over all N occupied ones, $\psi_i(\vec{r})$. This quantity represents the probability density of finding an electron at position $\vec{r}$ and is normalized such that $\int \rho(\vec{r})d\vec{r} = N$ (total number of electrons).

The momentum-space orbitals (momentals) can be computed from position-space orbitals via the three-dimensional Fourier transformation:

$$\phi_i(\vec{p}) = (2\pi)^{-3/2} \int \exp(-i\vec{p} \cdot \vec{r})\psi_i(\vec{r})d\vec{r} \tag{2}$$

From these momentum-space orbitals, the total momentum-space density is constructed as

$$\gamma(\vec{p}) = \sum_{i=1}^{N} |\phi_i(\vec{p})|^2 \tag{3}$$

This represents the probability density in momentum space, normalized such that $\int \gamma(\vec{p})d\vec{p} = N$.

Both representations are complete descriptions of the one-electron density and contain equivalent information about the electronic structure, related by the Fourier transform. The choice of representation reveals different physical aspects: position space emphasizes spatial localization of electrons, while momentum space emphasizes their kinetic energy distribution. Atomic units are employed throughout this work.

We have well-documented methods for Fourier transforming position-space orbitals based on ab initio calculations [56], given the linearization of atomic basis functions and the availability of analytical Fourier transforms of atomic basis functions as given in [57]. Note also that it is computationally feasible to transform full molecular electronic wave functions from the position to the momentum space in ab initio orbitals [58].

3.2. Shannon Entropy

The delocalization of the electron density in the molecular configuration space can be quantified through the Shannon entropy S. In terms of being a unit-normalized probability density in position space, it can be expressed by the logarithmic functional [59]:

$$S[\rho] = -\int \rho(\vec{r}) \ln \rho(\vec{r})d\vec{r} \tag{4}$$

This parameter has a maximum value if the information on $\rho(\vec{r})$ is small and our distribution is delocalized. This indicates that as electronic distributions become more diffuse, they exhibit increasingly higher entropy. The Shannon entropy in position space behaves like a measure of delocalization or lack of structure of the electronic density in the position space and hence is maximal when the knowledge of $\rho(\vec{r})$ is minimal and becomes delocalized. The Shannon entropy in momentum space S_p is largest for systems with electrons of higher speed (delocalized $\gamma(\vec{p})$) and is smaller for relaxed systems where kinetic energy is low. The units of Shannon entropy depend entirely on the logarithm base used in its definition, i.e., $\log_2$ for bits, $\log_e$ for nats, and $\log_{10}$ for dits.

3.3. Fisher Information

The Fisher information is a functional of the gradient of the electron density, defined with respect to the spatial point-wise probability distribution of the electronic cloud [60,61]:

$$I[\rho] = \int \frac{|\vec{\nabla}\rho(\vec{r})|^2}{\rho(\vec{r})} d\vec{r} \tag{5}$$

The position Fisher information I_r, closely linked to kinetic energy [62], serves as a measure of the spreading of electron density throughout space, exhibiting a local character due to its dependence on the gradient of the electron density. Unlike the Shannon entropy, which represents a global measure of spreading, the position Fisher information gauges the spatial concentration of the electronic probability cloud at individual points, providing a quantitative assessment of density irregularities and the intensity of its oscillatory behavior. Consequently, it exhibits high sensitivity to electronic fluctuations, enabling precise exploration of changes in electronic distributions. Fisher information has units of inverse length squared L^{-2}.

3.4. Disequilibrium

The information entropy [63], variances and variabilities of self-similarity [64] in the probability density are expressed in D, known as the disequilibrium. For position space, it is expressed as

$$D[\rho] = \int \rho^2(\vec{r}) d\vec{r} \tag{6}$$

Greater non-uniformity in the charge distribution is associated with a larger disequilibrium, which quantifies the departure of the probability density from uniformity. Disequilibrium has units of L^{-6}.

3.5. Complexity Measures

Quantifying (physical) system complexity (aside from specific entropic measures) makes it easier to evaluate structural organization. We employ two complementary complexity measures comprising alternate information-theoretic quantities. Our López–Ruiz–Mancini–Calbet (LMC) complexity measure [65,66] is a combination of disequilibrium and Shannon exponential entropy:

$$C_{LMC} = D[\rho] \cdot e^{S[\rho]} \tag{7}$$

Such a measure captures the balance between the uniformity (disequilibrium) and the disorder (entropy) of the electron density and the coordination of the electron density owing to the complex intrinsic structural features of the electron density (disequilibrium). For any three-dimensional probability density, the parameter satisfies the constraint $C_{LMC} \geq 1$. The Fisher–Shannon (FS) complexity measure, in turn, combines the following local and global information functionals [67,68]:

$$C_{FS} = I[\rho] \cdot J[\rho] \tag{8}$$

where $J[\rho] = \frac{1}{2\pi e} e^{\frac{2}{3}S[\rho]}$ is Shannon power entropy. This parameter demonstrates the existence of either localized or delocalized features of the electron density. It meets the lower bound $C_{FS} \geq 3$ of any 3D probability density. This complexity metric is dimensionless, invariant under replication, translation, and scaling transformations [69], and has few values for the extremes of probability distributions (ordered none, extreme disorder). All measures listed above are inherently generalizable to momentum space with the corresponding momentum density $\gamma(\vec{p})$ and, therefore, serve as complementary functionals of both kinetic energy distributions and nuclear motion effects.

4. Approaches to Evaluate Group Separability

Two statistical analyses were conducted to determine if the 3D span formed by the Shannon–Fisher–disequilibrium triads in position and momentum spaces is characteristic of common element types. Elements were divided by period, group number, chemical families (e.g., alkali, halogens, noble gases, etc.) and blocks (s, p, d, f). For each of the classifications, such analyses were done based on the triads in both position and momentum spaces. Moreover, in order to decrease the impact of different scales of the IT measures, Min–Max normalization was conducted. This procedure was performed by subtracting the minimum and dividing by the range (the difference between the high and low).

To test class separability in the IT space, we calculated Wilks' Lambda statistic (Λ) [70]. From the perspective of multivariate analysis of variance (MANOVA), Λ is the ratio of the within-group variance to the total variance and was computed by the determinants of error (E) and hypothesis (H) matrices: $\Lambda = |E|/|E + H|$. In general terms, E is the sum of the within-group squares and cross-products (SSCP) and H is the between-group SSCP. In simple terms, this statistic indicates group overlap along the multi-dimensional space; values close to zero indicate that the three IT measures distinguish the classified groups sufficiently well. Wilks' lambda calculations were done with the statsmodels python package [71].

In a similar vein, the random forest algorithm was applied [72] to test how accurate the element classifications could be recovered from the IT triad. Random Forest is based on making an ensemble of decision trees; therefore, the high classification accuracy proves that the IT features have a considerable discriminative power in respect to one chemical classification. Model performance was assessed using five-fold cross-validation. This arrangement consisted of five independent models, each trained on 80% of the data while the remaining 20% was used for validation in a rotating manner. The average accuracy (corresponding to the correct predictions divided by the total number of elements) was employed as a test result in order to measure the relation between the IT triad and the classifications. All computations were performed with the implementation offered for the scikit-learn library [73].

5. Results and Discussion

5.1. Shannon Entropy Perspective of the Periodic Table

Shannon entropy decreases gradually with increasing atomic number, illustrating a global trend of increasing electronic localization with nuclear charge (Figure 1). Every period has its own colored curve, and the steplike patterns correspond with the periodic filling of the electron shells. High Shannon values ($Z < 10$) in light elements appear due to diffuse, hydrogen-like orbitals with wide probability distributions. The stronger the Coulomb attraction, the more compressed the electron density will be and, with the rise of Z, the smaller the Shannon entropy.

The local discontinuities on the Shannon curve are the beginning or the end of each period: entropy increases at the beginning of a new shell (Li, Na, K), then declines uniformly, as a shell fills. Transition-metal regions exhibit flatter behaviors, indicative of d-orbital contraction and enhanced electron-density localization. Above $Z \approx 60$, the entropy values stabilize around ≈1.0, revealing a high-density regime of close-packed electron distributions characterized by strong relativistic and screening effects. The plot also depicts the information-theoretic imprint of periodicity, which constitutes shell structure, sub-shell filling and the stepwise confinement of atomic electron densities in the periodic table as we discuss below.

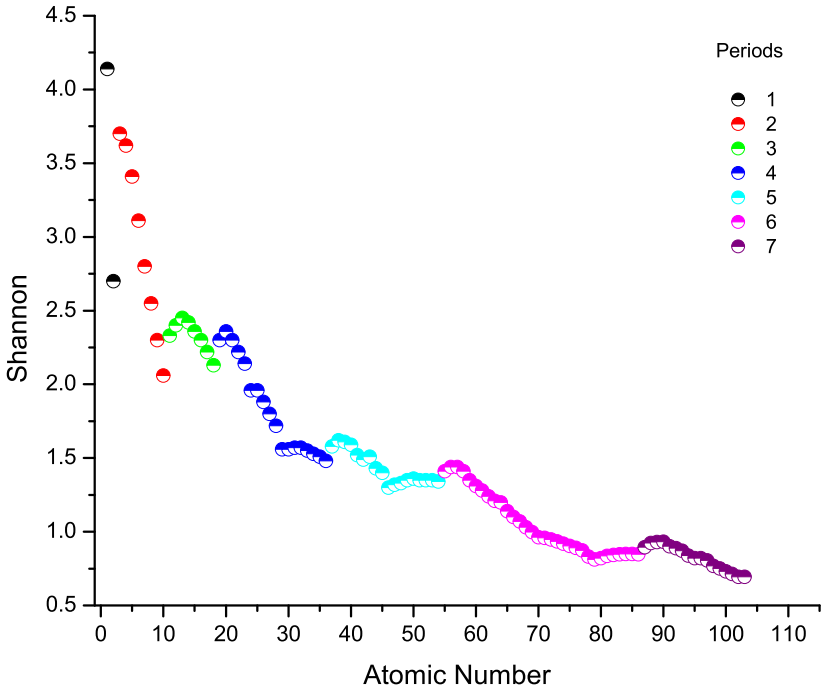

Figure 1. Shannon entropy in position space vs atomic number of atomic elements from 1 to 103. Periods are displayed in a particular color, demonstrating the decreasing entropy as nuclear charge increases.

Orbital-Resolved Analysis of Shannon Entropy Trends

The Shannon entropy profile in Figure 1 reveals distinct behaviors for different $n\ell$ orbital series, reflecting the interplay between nuclear attraction, electron shielding, and orbital penetration. We briefly analyze these trends:

***s*-orbital series.** The 1s series (H $\rightarrow$ He) exhibits a steep entropy decrease because these electrons experience the full nuclear charge with no shielding; adding the second electron significantly contracts the distribution. The 2s series (Li $\rightarrow$ Be) shows a more moderate decrease due to partial shielding by the 1s core combined with the 2s orbital's penetration toward the nucleus. For the outer s series (3s–6s), the trend reverses: these orbitals lie outside substantial core regions, and increasing the shielding from inner shells partially compensates the growing nuclear charge, resulting in progressively more diffuse outer s electrons and thus increasing entropy within each series.

***p*-orbital series.** The 2p series displays the steepest entropy decrease due to direct exposure to increasing effective nuclear charge with minimal shielding. Higher p series (3p–6p) experience progressively greater shielding from both core electrons and same-shell s electrons, producing flatter trends.

***d*-orbital series.** The d orbitals are substantially shielded by inner s and p shells. The 3d series exhibits the greatest variation due to the well-known "3d collapse" phenomenon, wherein poor shielding by 3p electrons leads to significant contraction across the first transition series. The 4d and 5d series, benefiting from more effective shielding, display more uniform behavior.

***f*-orbital series.** The similarity between the 4f (lanthanide) and 5f (actinide) series reflects the deeply buried nature of f orbitals within the atomic core. These electrons experience relatively uniform effective nuclear charges across each series. The "lanthanide contraction" affects both series similarly, producing nearly parallel entropy profiles.

These orbital-specific trends demonstrate that the information-theoretic measures are sensitive to the detailed physics of electronic structure, capturing effects such as shielding, penetration, and orbital collapse that underlie the organization of the periodic table.

5.2. Fisher Across the Periodic Table

Fisher information is almost monotonic and also strongly growing with atomic number, thereby indicating that the electronic probability density increases and sharpens with increasing atomic charge (Figure 2). Fisher information is strongly sensitive to local gradients of the electron density. When Z is greater, the Coulomb attraction remains stronger leading to less diffuse densities and more shell structural changes, hence higher values indicate sharper, more localized electronic features with steep gradients due to the compression of the electronic cloud near the nucleus. Unlike the steeply periodic behavior of Shannon entropy—which decreases with increasing atomic number and manifests strong periodic modulations— Fisher information displays an almost linear trend, increasing with atomic size as the shell structure augments.

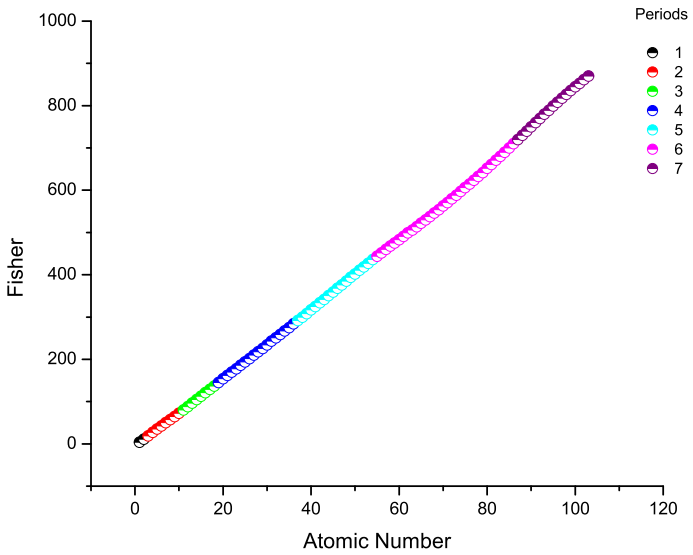

Figure 2. Fisher measurement in position space vs atomic number of atomic elements, from 1 to 103.

The period–colored points proceed along a smooth nearly piecewise–linear trajectory, suggesting that Fisher information is mainly affected by global nuclear charges versus shell structure. These inflection points at the early half of each period correspond to an introduction of a new principal quantum number—however, these deviations correspond to inflection points far below the overall increase. The transition, lanthanide, and actinide regions continue this gradual increase, while adding d and f electrons makes a new density gradient without any major deviation from the global trend, which is also apparent at the transition and lanthanide regions. On the whole, the plot indicates that, from an information-theoretic standpoint, Fisher information serves as a sensitive surrogate for electron-density localization, where the radial tightening of atomic distributions across the periodic table can be taken as an approximation of the Shannon entropy.

5.3. Disequilibrium Through the Periodic Table

The disequilibrium measurement is linearly increasing with atomic number, indicating a growing divergence of atomic electron densities (from a uniform or maximally delocalized distribution) (Figure 3). Because increased nuclear charge causes the electron cloud to become more compact and to be organized around the nucleus, it raises the probability concentration near certain regions in space, which in turn raises the level of disequilibrium.

The plot exhibits a nearly continuous convex trend in the upper right quadrant, with only some minor perturbations in the beginning of each period, suggesting that the dynamics of disequilibrium are primarily driven by the global confinement effects of shell or sub-shell structure.

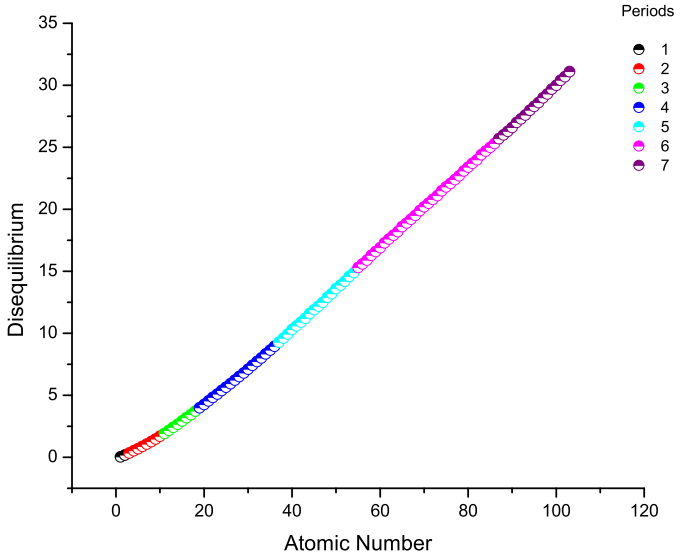

Figure 3. Disequilibrium measure in position space versus atomic number of atomic elements from 1 to 103.

While Shannon entropy decreases and Fisher information rises sharply with Z, disequilibrium evolves more moderately, capturing the increasing spatial order and concentration associated with heavier atoms. The colored points show that all periods follow a common trajectory, with successive periods merging seamlessly into the same curve, further emphasizing that disequilibrium behaves primarily as a measure of global electron-density non-uniformity. Overall, the figure highlights the monotonic organization of atomic structure in information-theoretic terms: higher-Z atoms display progressively greater departure from uniformity, consistent with stronger Coulomb binding and higher electronic localization.

5.4. Relationships Between Information-Theoretic Measures

5.4.1. Shannon Entropy and Disequilibrium Comparison

Shannon entropy and disequilibrium change in an opposite manner across the periodic table (Figure 4): elements with greater dispersive electron densities (high Shannon) have less disequilibrium, whereas elements with greater structural concentration (higher disequilibrium) exhibit a lower Shannon. Thus, this information plane reveals how the electronic cloud is compressed as the atomic number increases. The early-period elements (H-Ne) occupy the upper-left region, owing to their diffused and weakly bound electron distributions, which allow high entropy and low disequilibrium. The expansion of Z results in a gradual displacement of points which shifts to the lower-right side, indicating local ordering as a consequence of augmented nuclear attraction.

The colored trajectories corresponding to different periods align along a common descending curve, showing that the Shannon–disequilibrium relationship is shell-dependent due to the modulations appearing at the onset of each new period. These features reflect subtle shell and sub-shell reorganizations—depicted by S—but showing an overall ascending monotonic trend—depicted by D, see Figure 3—as the atomic number increases. In information-theoretic terms, the diagram illustrates a fundamental complementarity: Shannon entropy captures global spread, while disequilibrium captures global homogene-

ity or uniformity; together they encode the systematic evolution of atomic electron densities across the periodic table.

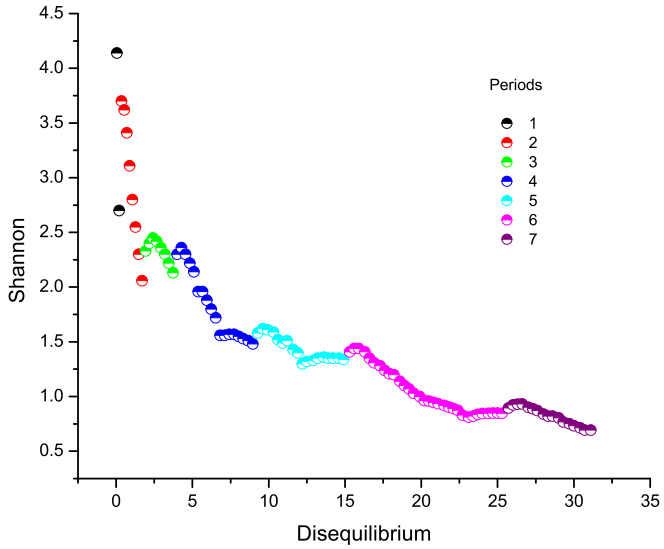

Figure 4. Shannon entropy and disequilibrium metric in position space for atomic elements from 1 to 103.

5.4.2. Fisher Information and Disequilibrium

The Fisher–disequilibrium plot shows a stable, smooth, and almost monotonic association of these two measures, indicating that both are sensitive to both the localization and the concentration of atomic electron density in a framework (Figure 5). With increasing disequilibrium and further perturbation of the uniform distribution, the Fisher information becomes more consistent by expressing more prominent spatial gradients associated with the stronger nuclear attraction at the higher atomic number. It looks moderately convex; it tends to expand toward the superlinear growing of electron-density gradients as atoms compress across the periodic table.

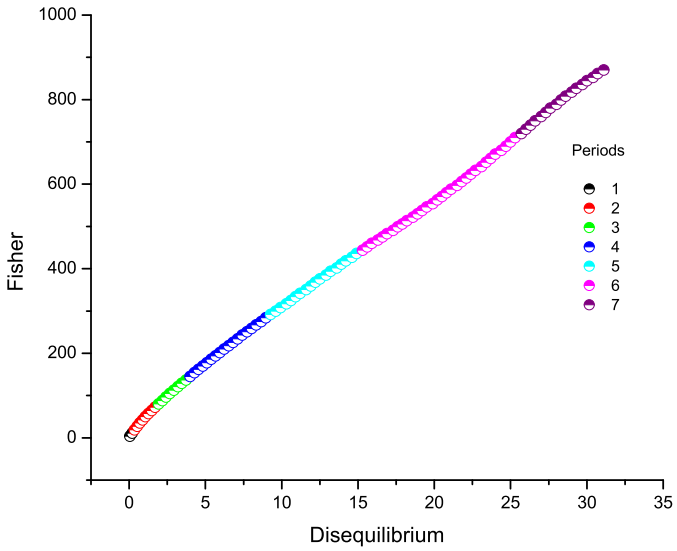

Figure 5. Fisher versus disequilibrium measure in position space for atomic elements 1 to 103.

Distinct periods track the global trajectory with only small deviations, so the Fisher–disequilibrium relation is actually really universal and shell independent. Shell onsets introduce slight departures from monotonicity, but the overall tendency remains consistent:

both parameters increase in proportion to the augment in nuclear charge. In the information-theoretical approach, the plot illustrates that Fisher information (a gradients-based measure) and disequilibrium (a global concentrations-based measure) reflect the localization of the atomic electron cloud and are complementary measurements of spatial order in the evolving structure of the periodic table.

5.4.3. Fisher Information Versus Shannon Entropy

The Fisher–Shannon plot shows a reverse relationship between global delocalization (Shannon entropy) and local gradient content (Fisher information) per period (Figure 6). The elements with relatively diffuse electron densities (for example, H and He) appear in the high Shannon–low Fisher region, reflecting delocalized probability distributions with low spatial organization. With expanding atomic number, points shift smoothly toward the low-Shannon/high-Fisher region, corresponding to the electronic cloud shrinking and sharpening as a consequence of the increment in nuclear charge.

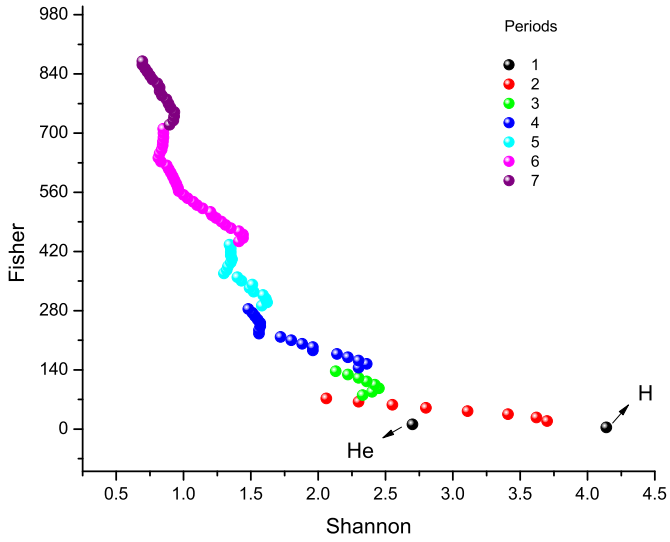

Figure 6. Fisher versus Shannon in position space for atomic elements 1 to 103.

The colored sequences follow very clear, continuous paths for the periods, with minor discontinuities for starting new shells. However, in practice, periods are generally in a downward trend, implying that the Fisher–Shannon relationship is effectively a common type of general behavior modulated by shell or sub-shells variations. This behavior is a sign of coupling between two indicators: Shannon entropy is the spatial extent and Fisher information is localization intensity and gradients. Their common pattern serves to indicate a systematic information-theoretic signature of the atomic structure: more Z implies that atoms are increasingly ordered, compact, and gradient rich—an overall common Fisher–Shannon structure.

5.5. Three-Dimensional Information-Theoretic Profile

5.5.1. Periodic Representation

The 3D plot of Shannon entropy, Fisher information, and disequilibrium shows a highly ordered and continuous helicoidal information-theoretic manifold that the chemical elements follow through the periodic table (Figure 7). Rather than forming dispersed or irregular clusters, the points align along a well-defined continuous trajectory. This trajectory increases primarily along the Fisher axis and toward the disequilibrium pole, with additional variations reflected in the Shannon dimension. This phenomenon is reflective of a fundamental shift in atomic electron density. Electron clouds grow more localized and

gradient-rich as nuclear charge increases, thus giving higher Fisher and disequilibrium values and decreasing their global propagation (Shannon). The helicoidal threefold structure in (Shannon, Fisher, disequilibrium) space might be more easily appreciated in the video abstract included in the Supplementary Materials. The use of the terminology is clarified below.

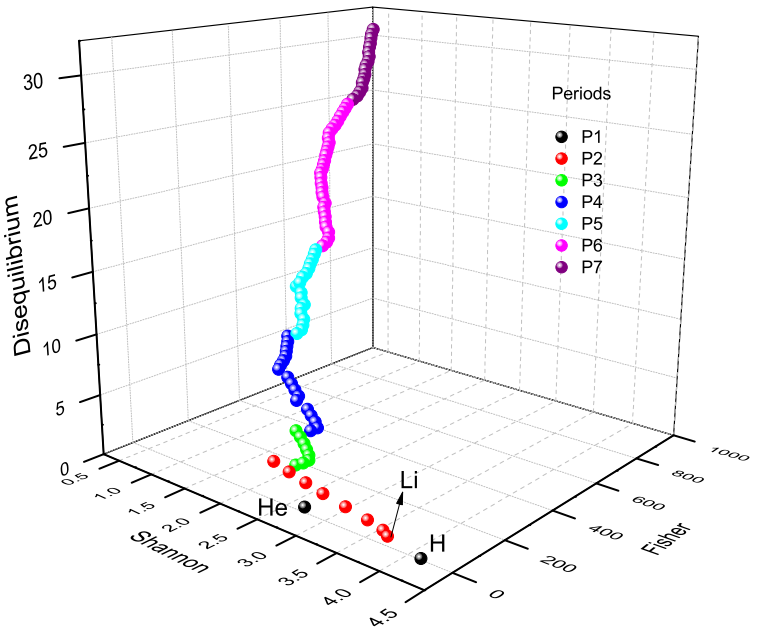

Figure 7. 3D graphical diagram of the disequilibrium–Fisher–Shannon information-theoretic components in position space of the atomic elements from 1 to 103 on the periodic representation of the periodic table. An animated rotation of this plot is included in the Supplementary Material.

Every period (color-coded) takes up a clear part of the 3D curve, and while tiny deviations show up at the beginning of each shell—manifesting as slight bends or kinks—on the whole, the geometry is formed into some information-theoretic helix-like shape or helicoidal. On the Shannon axis, each successive period shifts progressively towards lower entropy, along the Fisher axis they ascend through narrower density gradients, and on the disequilibrium axis they extend outwards with density concentration. Such movements produce a helicoidal pattern in information space, in accordance with earlier discussed models that described the periodic table as a circular or helix structure rather than a flat or horizontal tabular one. The current information-theoretic structure provides further quantitative support for such concepts, as it establishes that atomic structure develops smoothly and monotonically along a quasi-helical path in (Shannon, Fisher, disequilibrium) space, where noble gases function as regional turning points: He and Ne are shown to display characteristic inflection features that mark shell closures.

Importantly, the 3D trajectory is continuous and single-valued, which further supports the argument that information-theoretic measures capture periodicity as a coherent ordered evolution rather than an aggregation of discrete blocks. This gives one a unified framework that makes it possible to understand the periodic table as a helicoidal graph in the information space and encode the tradeoff between the global delocalization, the local structure and the probability concentration in each element's electronic architecture.

In the 3D representation given by Fisher–Shannon–disequilibrium, Periods 1 to 7 have a single continuous path along information-theoretic channels whereas each period has defined and identifiable segments on the global trajectory. The lower-disequilibrium, lower-Fisher, high-Shannon end of the curve is anchored on Period 1; hydrogen and helium demonstrate the most diffuse electron densities, which comprise the broad base of the

information helicoidal structure. Period 2 (Li–Ne) is the first great decline of Shannon entropy and the first definite increase in both Fisher information and disequilibrium, indicative of the completion of the 2*p* sub-shell, and provides the characteristic bend that starts the helical-like pathway. Period 3 (Na–Ar) moves the flow further down in Shannon and up in Fisher/disequilibrium along a nearly parallel (but displaced) route in which the information-theoretic order maintains a vertical level while new shells are inserted. Periods 4 and 5, which contain the 3*d* and 4*d* transition metals, present the most visible smooth mid-section of the helicoidal progression—where increased concentrations of Fisher information and disequilibrium become more apparent due to the growing localization and intensification of gradients owing to *d*-electrons. Their trajectories retain close alignment with the global curve, highlighting that—along with more complex sub-shell structures—electron-density localization increases monotonically with nuclear charge. Period 6 with lanthanides exhibits stronger clustering in Fisher along with disequilibrium, which translates to a steeper ascent in the 3D space as shown in the contraction of the *f*-electron filling, as well as higher localization. Period 7 continues from this angle, and stretches the helicoidal trajectory to its highest Fisher and disequilibrium values with lowest Shannon values, reflecting the most compact electron densities among all those known elements.

Collectively, the seven periods comprise an ordered set of information-theoretic loops, each shifted relative to the previous one along all three axes. This helix-like geometry provides quantitative support for the qualitative helical representations of the periodic table. The path of each period is similar in shape—representative of repeating shell structure—but displaced upward and inward in information space by the stronger nuclear attraction of heavier atoms. This is a straightforward indication that the famous periodicity of the elements appears almost naturally as a geometrical helicoidal structure in the 3D (Shannon, Fisher, and disequilibrium) space.

5.5.2. Clarification on the Use of the Term "Helicoidal Manifold"

In this work, the term helicoidal manifold is used in a descriptive and conceptual sense, rather than implying a rigid geometrical or differential–geometric construction. By a helicoidal manifold we mean a smooth, continuous, non-planar trajectory embedded in a three-dimensional information-theoretic space, whose global organization combines a monotonic progression along one direction with a systematic rotational or torsional displacement along the others. Specifically, the manifold is defined by the ordered mapping of atomic elements (Z = 1–103) into the three-dimensional space spanned by Shannon entropy, Fisher information, and disequilibrium. As the atomic number increases, the trajectory evolves continuously without self-intersections, exhibiting a global translation driven by increasing localization and concentration of the electron density, together with periodic modulations associated with shell and sub-shell structure. These combined features give rise to a helix-like or helicoidal organization in information space.

Importantly, the use of the term "helicoidal" does not imply constant radius, constant pitch, or exact cylindrical symmetry. Instead, both curvature and torsion vary smoothly along the trajectory, reflecting the non-uniform influence of electronic shell filling, screening, and orbital contraction across the periodic table. The helicoidal geometry therefore emerges naturally from the information-theoretic measures themselves and is not imposed a priori by any assumed geometric model. In this context, the word "manifold" is employed to emphasize the continuity, smoothness, and single-valued character of the trajectory in information space, rather than to invoke a formal metric or topological structure. The helicoidal manifold thus provides a compact and physically meaningful representation of atomic periodicity as an emergent geometric organization arising from the monotonic and periodic evolution of information-theoretic descriptors.

5.5.3. Block Representation

Each block (s, p, d, f) occupies a discrete, contiguous territory in the global information-theoretic trajectory (Figure 8), providing a clear indication of how orbital symmetries can be realized as a clear defined portion of information space.

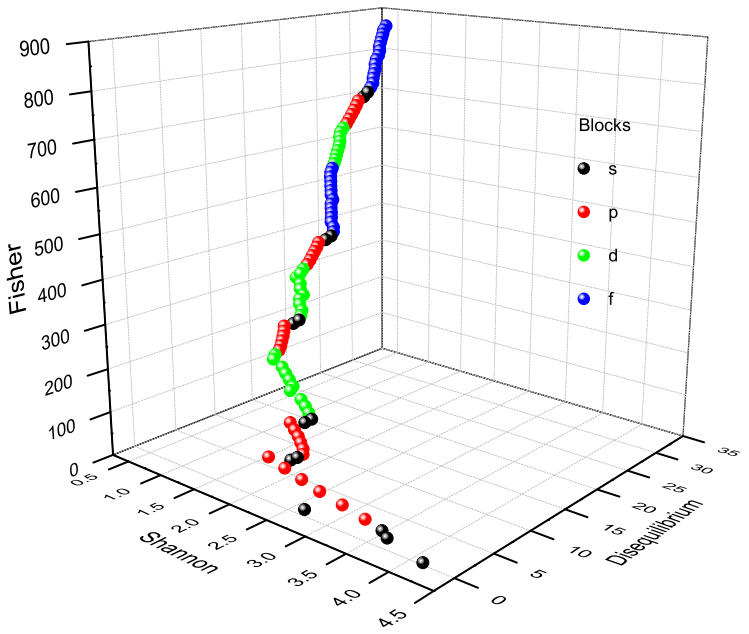

Figure 8. 3D Graphical View of disequilibrium–Fisher–Shannon information-theoretic components in position space for atomic elements from 1 to 103: block representation of the periodic table.

The s-block (black points) is the high-Shannon, low-Fisher, low-disequilibrium edge of the curve, which is grounded on hydrogen and helium. Due to their sparse gradient content (Fisher) and low disequilibrium, these elements have the most diffused and least structured electron densities. As s-block atoms become heavier (alkali and alkaline-earth metals), they show modest increases on Fisher and disequilibrium scales, but relatively high Shannon values persist, in contrast to those of single- or dual-electron valence configurations and spherical symmetry.

The p-block (red points) appears as a well-defined middle point on the 3D course. As electrons occupy directional p-orbitals, the electron density becomes increasingly more anisotropic and a more defined structure is established, which also moves the p-block to become higher in Fisher information and disequilibrium and lower Shannon entropy. The curvature of the p-block path is smoother than that of the s-block, because the localization response is more systematic as the number of the p-electrons increases.

The d-block (green points) shows a very prominent upward migration along the Fisher and disequilibrium axis. The d-electrons, more localized and more strongly affected by the increasing nuclear charge, produce denser gradients and a higher spatial density. Thus, the d-block takes up a vertically high part of the information manifold, with minimal deviation from s- and p-blocks. The transition metals continue through the segments, with those segments experiencing the largest differences in the 3D trajectory, confirming the stronger information-theoretic impression of d-orbital filling.

Among all blocks, the f-block (blue points) reaches the maximum Fisher and disequilibrium and lowest Shannon entropies. Such f-electrons are tightly coupled, contracted with strong resistance, and extremely sensitive to expanding Z, offering high localization and high density gradients. In contrast, the f-block is the top part of the 3D helicoidal curve, with a longer vertical climb for Fisher-disequilibrium dimensions. The former is

also common in lanthanides and actinides where it is the effect of f-orbital contraction and relativistic effects that dominate electronic structure at this point, although the latter effect is not directly represented here.

The four blocks, when viewed together, represent a layered, ascending process in information space, wherein $s \rightarrow p \rightarrow d \rightarrow f$ denotes a sequential increase in both localization and structural complexity of the electron density. The 3D rendering makes this evolution visually explicit: each block maps on a different region of the Fisher–Shannon–disequilibrium manifold and so provides a quantitative information-theoretic fingerprint of orbital symmetry and electronic organization along the periodic table.

5.6. Information-Theoretic Significance of Chemical Anomalies

The previous analyses motivate further examination of the Shannon–disequilibrium plots of Periods 2, 3, and 4: these plots exhibit faint but chemically significant and quirkier deviations from the formation of atomic electron densities (anomalies) along the periodic table (Figure 9). Overall, for all periods, a constant decrease in Shannon entropy is evident in each period, indicative of gradual localization of electron density and an increase in disequilibrium. This provides evidence that, as Z increases, there is a general shift from uniformity in equilibrium towards increased inhomogeneity. But anomalies occurring in Periods 2–4 are especially noteworthy (Figure 9). Nevertheless, this behavior does diverge from the strict monotony of phases with which they are known, and these deviations are well in line with common chemical anomalies in orbital filling and electron-shell construction.

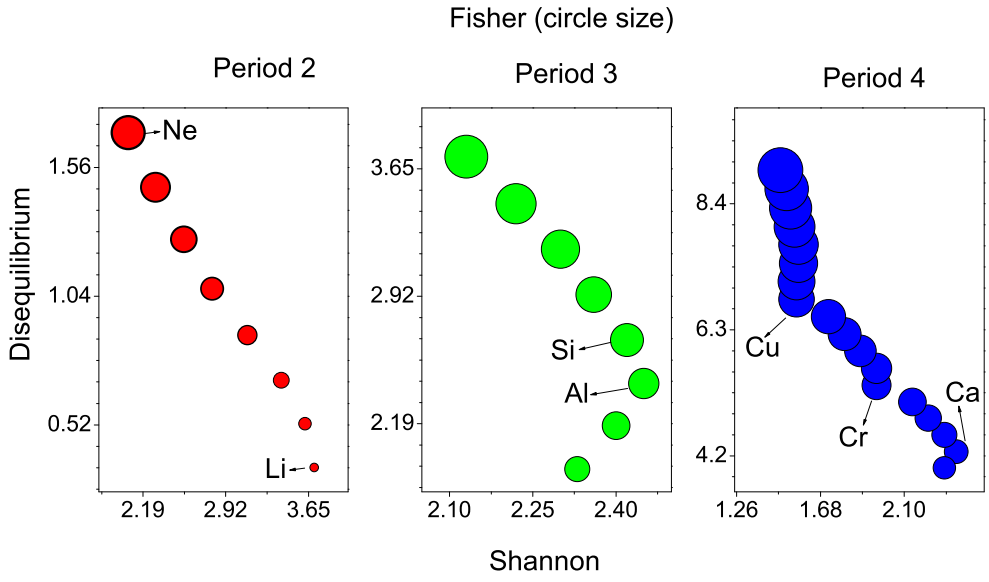

Figure 9. Situation space analysis of the disequilibrium–Shannon representation for Periods 2, 3, and 4, showing the chemical anomalies caused by information-theoretic nuclear elements. Marker sizes are scaled by Fisher information.

In particular, from Period 2 (Li–Ne) onwards, the smooth Li transition to Ne is interrupted at the p-block initiation (B, C) where increasing angular geometry associated with partial p-electron occupancy yields points slightly off the idealized curve. Neon, with its closed $2p^6$ shell, exhibits characteristically low Shannon entropy (reflecting strong electronic localization due to effective nuclear confinement) combined with high Fisher information, evidenced by the larger circle size (reflecting sharp density gradients at the shell boundary). This information-theoretic signature is consistent with neon's unique role as a noble gas: its closed-shell configuration creates both spatial compression (low Shannon) and steep den-

sity gradients (high Fisher), which together constitute an information-theoretic fingerprint of noble-gas closure and shell completion.

In Period 3 (Na–Ar), Si stands out as a clear anomaly: its Shannon–disequilibrium position deviates slightly upward from the smooth descending trend. This reflects the exceptional bonding versatility and intermediate localization of the $3p^2$ configuration, which is also expressed chemically in Si's ability to form extended covalent networks (silicates, polysilanes). This information-theoretic deviation parallels its well-known position as a chemically central element in the *p*-block.

One of the most interesting anomalies happens at Period 4 (K–Kr), showing transition-metal disjoints that are producing a fine information-theoretic signal. A half-filled $3d^5 4s^1$ structure composed of chromium moves up to a higher Shannon and tends to be reduced lower towards the equi-dimensionality value in neighbouring atoms at relatively close distances. This is attributed to its superdelocalized and symmetric electron balance, as would predict the stability of half-filled d sub-shell. Copper exhibits the anomalous $3d^{10}4s^1$ arrangement and is found further down the Shannon axis than expected (relative to the global decreasing trend), which may indicate its proximity to the filled d shell, i.e., the more localized it is. This information-theoretic dip is a property consistent with chemical behavior of Cu—which has high ionization and an excellent +1/+2 oxidation-state plasticity. Calcium is not indeed anomalous, but it occupies an orbital-filling area and shows a strong relationship between the *s*-block delocalization of the early $3d$ components and their increasingly local positions. As a result, Shannon entropy is relatively large while the disequilibrium remains relatively small, making this an indispensable anchor point for the period.

The anomalies observed in the information-theoretic analysis for Cr, Cu, Si, and Ne are not merely numerical deviations; they directly reflect the underlying electronic structure irregularities that determine chemical behavior. This section emphasizes that the information-theoretic descriptors we employ are sensitive probes of chemical phenomena.

Electron Configuration Anomalies: Chromium's anomalous $3d^5 4s^1$ configuration (instead of the expected $3d^4 4s^2$ produces a measurable signature in the Shannon entropy vs. disequilibrium plane, appearing at a lower Shannon value compared to the global trend. This anomaly arises from electron–electron repulsion and exchange stabilization effects that favor the half-filled d^5 configuration. Copper similarly exhibits the $3d^{10}4s^1$ configuration (full *d*-shell plus one *s* electron), which produces a characteristic information-theoretic signature distinct from surrounding transition metals.

Shell Closure Effects: Neon ($2p^6$), argon ($3p^6$), and other noble gases show distinctive information-theoretic signatures that mark the completion of electron shells, characterized by low Shannon entropy and sharp transitions in Fisher information.

Metal–Nonmetal Transition: Silicon's position as the boundary between metallic and nonmetallic character manifests as an informational anomaly in the *p*-block, reflecting its intermediate bonding character (metallic, covalent, and network-forming properties).

The key finding is that information-theoretic measures provide quantitative, physics-based descriptors of these chemical phenomena without requiring prior knowledge of chemical behavior. This demonstrates the utility of IT analysis as an independent tool for identifying and characterizing electronic structure anomalies across the periodic system.

To validate this interpretation, we note that the anomalies identified by IT analysis correspond precisely with well-documented chemical peculiarities: Cr and Cu show unusual oxidation states and reactivity; Ne, Ar, etc., show noble-gas character; Si shows amphoteric behavior. The convergence of IT signatures with chemical properties provides strong evidence that our information-theoretic descriptors are capturing fundamental aspects of atomic structure.

5.7. Triad Halogen Analysis

The 3D representation combining Shannon entropy, Fisher information, and disequilibrium provides a powerful geometric lens through which the triadic organization of chemically related elements can be examined (Figure 10). When focusing on the triads surrounding the halogens (Group 17)—specifically, (Group 1, Group 17, Group 18) blocks across different periods—three important insights emerge: hydrogen's ambiguous placement, the remarkable coherence within halogen–alkali–noble-gas triads, and the distinctive triangular cluster formed by the (H–He–Li) triad.

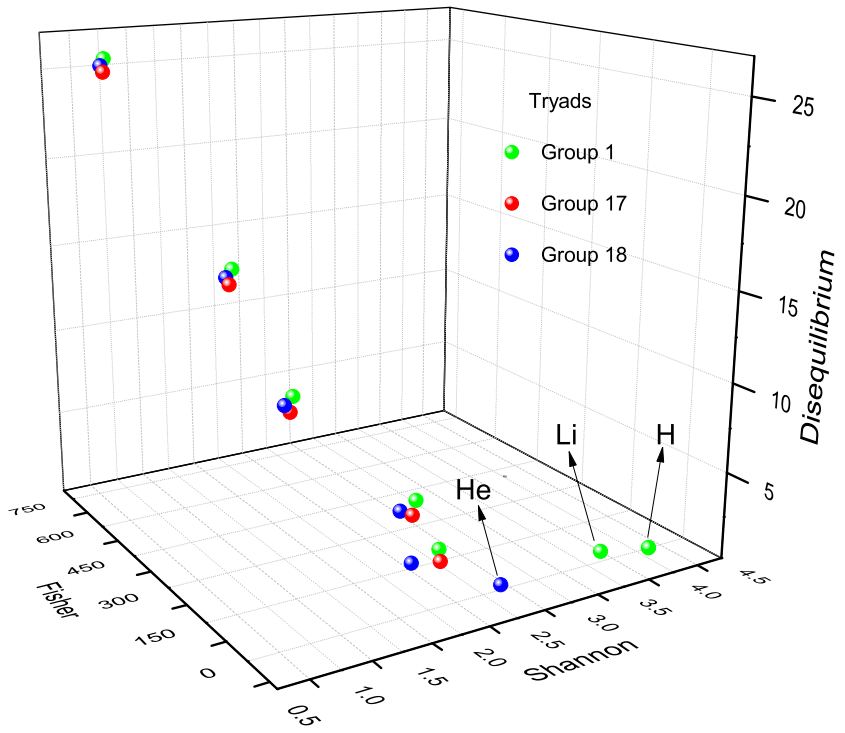

Figure 10. Using 3D graphical analysis of disequilibrium–Fisher–Shannon information-theoretic components in position space for the triadic elements surrounding the halogenic elements, indicating the similarities for hydrogen with Group 1 or Group 17 and unusual behavior by triad H-He-Li, including its similarity with the position space.

Three-dimensional information-theoretic coordinates for each triad (e.g., Li–F–Ne, Na–Cl–Ar, K–Br–Kr) create tight or quasi-equilateral triangular clusters. The Fisher (sharp gradients) and the disequilibrium (high localization) are both high in Group 17 (halogens), with electron density clusters being very compact, highly directional, and chemically reactive. Group 1 (alkali metals) exhibits the minimum Fisher and minimum disequilibrium (very delocalized densities), which leads to broad probability distributions of diffuse ns^1 valence electrons. Group 18 (noble gases) shows intermediate Fisher, intermediate Shannon and moderate disequilibrium, consistent with closed shell symmetrical phenomena of noble gases. Throughout all of the periods (2–6), these triads are structurally uniform in information-theoretic space—which identifies the universality of the periodic law of interest even when presented under an information-theoretic description.

The H–He–Li triad presents a fundamentally different pattern in the 3D Fisher–Shannon–disequilibrium manifold compared to the regular alkali–halogen–noble-gas triads of higher periods. Rather than forming a simple linear progression or regular triangle like triads in Periods 2–6 (Li–F–Ne, Na–Cl–Ar, etc.), the H–He–Li triad exhibits an asymmetric configuration reflecting the unique electronic simplicity and non-periodicity of Period 1.

Specifically, in position-space information-theoretic coordinates:

- Hydrogen: High Shannon entropy (diffuse 1*s* electron), low-to-moderate Fisher information (gradual density gradients), low disequilibrium (relatively uniform distribution).
- Helium: Lower Shannon entropy (two-electron shell effects cause some contraction), minimal Fisher information (smooth $1s^2$ density), very high disequilibrium (concentrated near nucleus).
- Lithium: Moderate Shannon entropy, moderate-to-high Fisher information (sharp peak in 2*s* electron density), high disequilibrium.

These three points do not form a collinear or triangular pattern; rather, they represent the transition from the extreme delocalization of H to the increasing localization of He and then the emergence of the 2*s* orbital in Li. This three-point arrangement is qualitatively distinct from the regular triadic patterns characteristic of higher-period elements, reflecting Period 1's non-periodic character. This demonstrates that H does not occupy a geometrically intermediate position between He and Li in this 3D manifold showing a different perspective on hydrogen's unique electronic structure.

We emphasize that these findings provide quantitative data bearing on the hydrogen placement question, but we do not advocate for any specific resolution. The 3D IT representation of the elements in position space aligns with the view that H does not belong to either the alkali metals or the halogens, but rather stands as a unique, stand-alone element. This particular positioning of hydrogen in IT space is a mathematical result that can inform the ongoing discussion among educators and philosophers of chemistry regarding optimal periodic table design.

5.8. Analysis of Complexity Measures

5.8.1. López–Mancini–Ruiz (LMC) Complexity

The 3D curve in Shannon–Fisher–disequilibrium space represents, yet again, the ordered information-theoretical evolution of the atoms. But when the LMC complexity is added as a fourth dimension using color coding (Figure 11), new insights are revealed. Low-Z elements (H, He, and light atoms of Period 2) are represented at the high-Shannon/low-Fisher/low-disequilibrium ends of the curve and are shaded purple. This means they have a low structural complexity: their electron densities may be either too broadly diffused (high entropy, low disequilibrium) or they are too simple. Consequently, there are not enough electrons to support a sufficiently rich internal structure. With increasing Z, points move up the length of the curve in a direction of larger Fisher and disequilibrium or smaller Shannon. The color gradually shifts from blue-green to orange or red as it goes.

Mid- and high-Z atoms (transition metals, lanthanides, and actinides) sit in the area of simultaneously large localization (high Fisher, high disequilibrium) and non-negligible Shannon entropy, the site where the LMC functional is at its maximum values. In other words, heavy atoms are not only more ordered (more localized) than light atoms; they are also more structurally complex, with a richer internal arrangement of the density of electrons. The color gradient around the single information-theoretic spine of the periodic table thus reflects a monotonic accumulation of atomic complexity from H to Lr, with relatively straightforward and weakly structured densities to the start but strongly organized and correlated densities to the finish, offering an attractive global representation of how the complexity of the atomic structure changes across the periodic table.

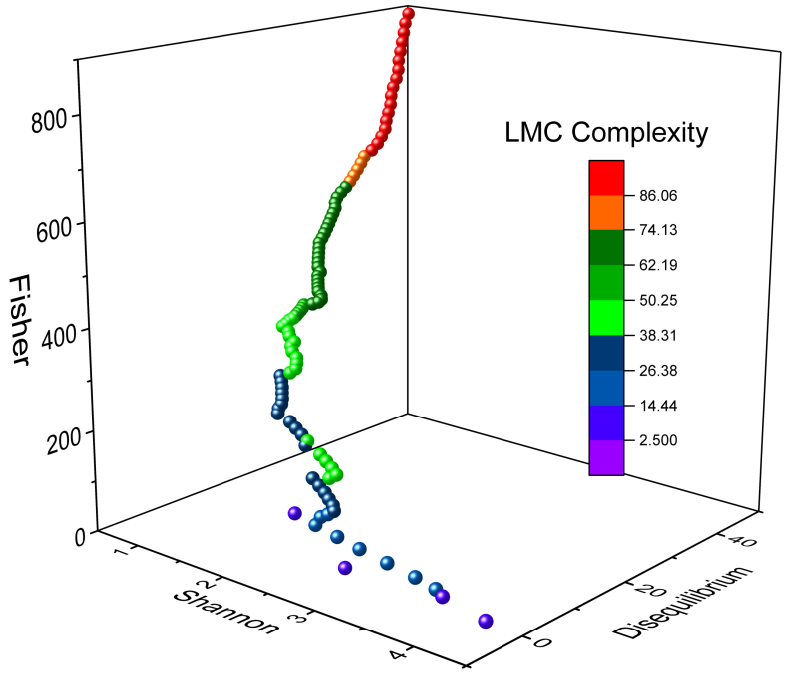

Figure 11. 3D visualization of disequilibrium–Fisher–Shannon information-theoretic components in position space of elements 1–103 with the López–Mancini–Ruiz (LMC) complexity with high/low colored code (reddish, bluish).

5.8.2. Fisher–Shannon (FS) Complexity

The information-theoretic backbone of the periodic table is plotted in 3D from H to Lr in the Shannon–Fisher–disequilibrium space of the atoms. When FS—a dyadic functional that combines global delocalization (Shannon entropy) and local sharpened structure (Fisher information)—is used to color this evolution, a monotonic curve emerges: complexity evolves uniformly in the periodic table (Figure 12).

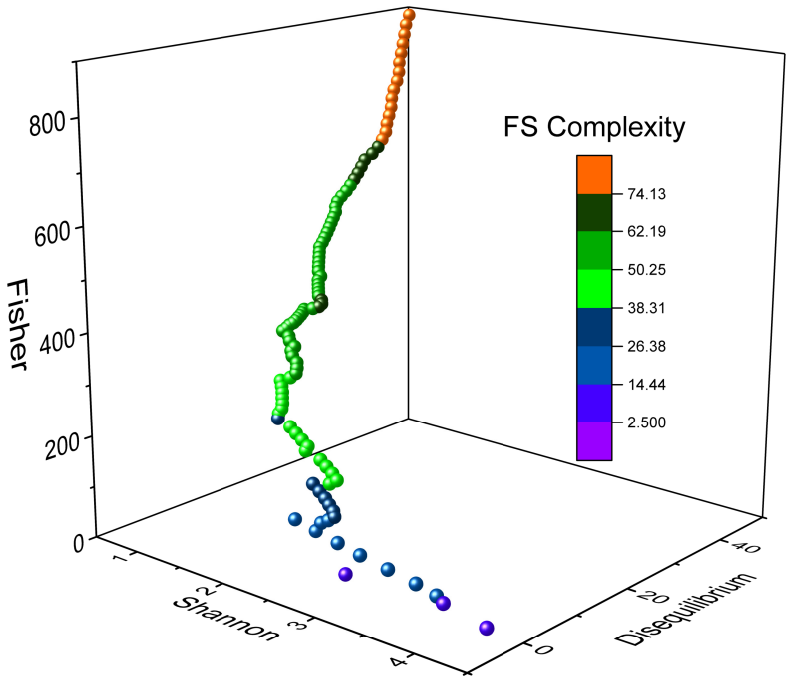

Figure 12. 3D plot showing disequilibrium–Fisher–Shannon information-theoretic components in position space in elements 1–103 with Fisher–Shannon (FS) complexity presented in color-coded levels (reddish/bluish).

In the purple-tinged high-Shannon/low-Fisher/low-disequilibrium end of the curve, the elements H, He, Li, Be, and B occur (low-complexity regime). Such atoms all have fairly elementary electron densities—either too diffusively dispersed (high entropy) or too symmetric to realize strong local gradients. In some of them, the FS functional is small, suggesting very few structural details in the information theory.

As Z increases in the second, third and fourth periods, the trajectory tends upward in Fisher, outward in disequilibrium and downward in Shannon. The colored range moves from blue to green (intermediate-complexity regime) due to the appearance of more organized electron densities, more pronounced when *p*- and early *d*-orbitals are populated. These atoms have a moderate global delocalization, but increasingly abrupt probability gradients, and cause the FS measure to increase.

Beyond $Z \approx 40$, especially within Periods 6 and 7, the Fisher and disequilibrium values increase substantially due to strong electron localization, while Shannon entropy stays large enough that nontrivial global spread is maintained. The most complex FS at these atoms (high-complexity regime) is shown in the deep orange region of the colored region. Late transition metals (Ru, Rh, Pd, Pt), lanthanides with *f*-electron contraction, and relativistic actinides tend to be clustering towards the upper deep green–orange region, being the richest and most complex electron density among all atoms.

Because FS complexity is multiplicative across Fisher and Shannon terms, it correlates positively with the color variation found here to correlate perfectly with the curvature of the 3D Fisher–Shannon–disequilibrium path. It is as a smooth informational helicoidal manifold, with rising Z rates resulting in a transition from purple to orange, which makes the periodic table appear as an exponential increase in structural complexity, leading to simple systems (H–Ne) appearing purple–blue, moderately structured systems (Na–Zn, Ga–Kr) taking on green, and highly complex systems (Zr–Lr) taking on deep green–orange. This is a basic information-theoretic law of the periodic system: atomic complexity increases monotonically with nuclear charge due to the combined increase in internal organization (Fisher) and nontrivial spread (Shannon) of electron density.

5.9. Momentum Space Analysis

The information-theoretic signature of the periodic table in momentum space is displayed through the 3D Fisher–Shannon–disequilibrium diagram, in contrast to its representation in position space, yet in a similar manner (Figure 13). In position space, the increasing localization of electron densities with Z is manifested, while momentum-space measurements reflect the corresponding inverse, complementary momentum delocalization (i.e., momentum broadening) associated with the uncertainty principle. This duality thus leads to a characteristic hierarchical configuration of the seven periods across the 3D manifold.

Hydrogen and helium (Period 1) are located at either end of this graph, with very high Shannon momentum entropy, and moderate Fisher momentum. Their diffused momentum distributions are typical of very compact real-space densities. Helium in particular demonstrates a sharp decrease in Fisher and high Shannon based on its highly symmetric compact $1s^2$ arrangement.

Period 2 (Li–Ne) is the most vertically clustered part of the diagram and contains the highest momentum-space Fisher information outliers. Lithium shows the largest value for the Fisher momentum due to its narrow peak-momentum distribution, which has much to do with its diffusing 2*s* electron in real space. Moving along Be $\rightarrow$ B $\rightarrow$ C $\rightarrow$ N $\rightarrow$ O $\rightarrow$ F $\rightarrow$ Ne, the points in Fisher decrease smoothly and shift towards the left in Shannon, in agreement with a contracting behavior of momentum-space distributions dependent on increased nuclear charge and contracting real-space densities.

Period 3 (Na–Ar) atoms occupy a lower, more compressed region of the 3D plot, representing narrower variability in momentum-space information-theoretic quantities. Their Fisher and Shannon values are significantly lower than those of Period 2, indicating more uniform momentum distributions. This reflects the stabilized 3*s* and 3*p* shells, where real-space contraction reduces momentum-space structure. Neon and argon define a nearly linear trend between Fisher and Shannon momentum, marking noble-gas closure.

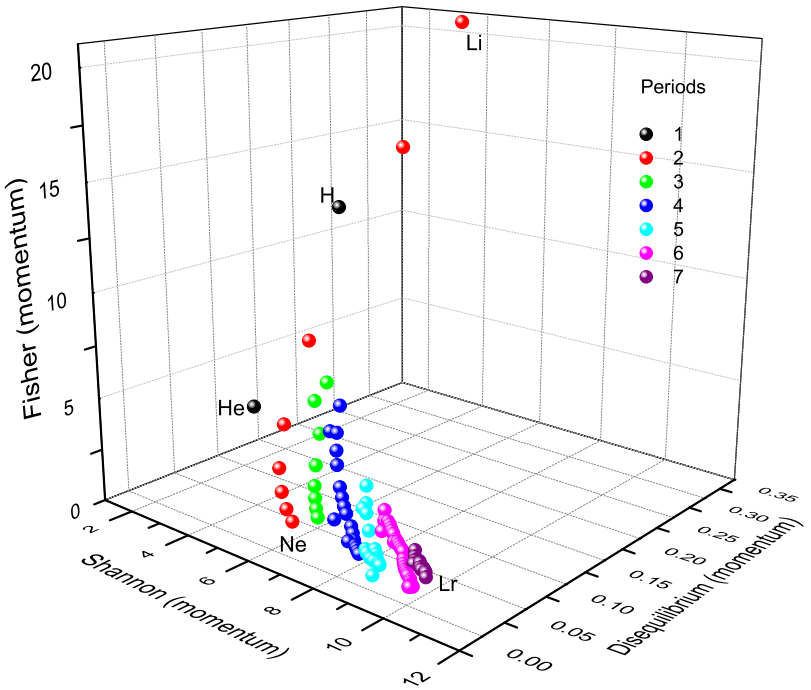

Figure 13. 3D graphical analysis of disequilibrium–Fisher–Shannon information-theoretic components in momentum space of atomic elements from 1 to 103, the periodic representation (1 to 7) of the periodic table.

Period 4 (K–Kr) exhibits a dense vertical short cluster, relatively low Fisher and high Shannon, compared to Periods 2 and 3. The relatively small change in Fisher's momentum space of the 3*d* elements demonstrates the real space effect, even with added complexity, via *d*-orbital contributors results in a more continuous, as well as a more moderate momentum distribution than in the two earlier periods. This is consistent with the delocalized angular elements in *d*-orbitals.

Periods 5–7 of the 3D manifold are the lowest. At low Fisher (approximately the 0–5 scale) and moderate disequilibrium they form a flattened, heavily overlapped cluster with gradually increasing Shannon momentum through different periods. This astounding collapse of information-theoretic structure in momentum space presents a significant real-space contraction (big Z), extreme relativistic changes in heavy members, and larger momentum distributions, which diminish Fisher information. Importantly, the concluding element (Lr) brings the trajectory to a halt at large Shannon momentum, suggesting that momentum distributions are diffuse due to highly relativistic, compact real-space densities.

We witness a stratified architecture of momentum-space information-theoretic components across the seven periods, particularly Period 2, which shows the maximum values of Fisher momentum and widest dispersion; Periods 3 and 4 which compress into compact structures; Periods 5–7 that collapse dynamically into narrow zones, confirming that heavy atoms share a remarkably similar momentum-space information-theoretic signature; and noble gases (He, Ne, Ar, Kr, Xe, Rn) creating the smoothest period-to-period alignments, as per closed-shell symmetry. Therefore, this organization constructs a vertical sequence

of periods, with the height (Fisher momentum) decreasing progressively from Period 2 to Period 7.

Another strong complementary image of periodicity is the 3D Fisher–Shannon–disequilibrium model in momentum space. While spatial position reflects rising localization with Z, momentum space reflects peak information-theoretic specification for lighter atoms (Periods 1–3), compression and similarity among heavier atoms (Periods 5–7), and distinct momentum-space fingerprints of shell closure and period bounding. This provides a coherent, information-theoretic map of periodicity describing both quantum-mechanical complementarity and classical chemical periodic patterns.

A Critical Finding: Hydrogen's Position in Momentum Space

The momentum-space analysis reveals a striking and significant result that merits careful discussion: hydrogen occupies an intermediate position between helium and lithium in momentum-space information-theoretic coordinates, in sharp contrast to its non-intermediate position in position-space coordinates (Section 5.7, Figure 10).

This is a profound finding with important implications for understanding hydrogen's role in the periodic system. To understand this result, we must consider the fundamental complementarity between position and momentum representations: the uncertainty principle requires that distributions diffuse in position space must be concentrated in momentum space, and vice versa.

In position space, hydrogen's 1*s* electron is highly diffuse, producing high Shannon entropy. Helium's closed-shell $1s^2$ is compact, producing low Shannon and high disequilibrium. In momentum space, by contrast, the situation inverts: a diffuse position-space distribution corresponds to concentrated momentum distribution (low-momentum spread), while a compact position-space distribution corresponds to a diffuse momentum-space distribution (high-momentum spread).

Therefore, in momentum space:

- Helium shows very low Shannon momentum entropy (electrons confined to low kinetic energies), very low Fisher momentum (smooth momentum distribution), very high disequilibrium momentum;
- Hydrogen shows intermediate Shannon momentum, intermediate Fisher momentum, and intermediate disequilibrium momentum;
- Lithium shows higher Shannon momentum entropy (2*s* electron has higher kinetic energy spread), moderate Fisher momentum, and moderate disequilibrium momentum.

This arrangement places hydrogen geometrically between helium and lithium in momentum-space information-theoretic coordinates (Figure 13), forming a regular geometric progression unlike the asymmetric position-space arrangement.

Physical Interpretation: This finding suggests that from the perspective of kinetic energy distribution and momentum-space electronic structure, hydrogen occupies a natural intermediate position between noble gases (low kinetic energy, tightly bound) and alkali metals (higher kinetic energy, more loosely bound). While position-space analysis emphasizes hydrogen's unique spatial delocalization, momentum-space analysis reveals that its characteristic kinetic energy places it between the kinetic extremes represented by He and Li.

Implications for Periodic Table Design: This result is potentially significant for ongoing discussions about optimal periodic table representations. Traditional position-space-based approaches suggest hydrogen's uniqueness and ambiguous placement. However, the momentum-space information-theoretic perspective suggests that hydrogen fits into a natural periodic sequence when kinetic energy structure is considered. This does not resolve the debate about hydrogen's optimal position, but it provides a new quantitative

argument from a complementary perspective. Different representations (position-space vs. momentum-space, real-space vs. reciprocal-space) may be most appropriate for different chemical questions.

The fact that the same atom appears in geometrically different positions in position and momentum space—and yet both perspectives are equally valid representations of the same electronic structure—illuminates the fundamental complexity of element classification. It demonstrates that no single representation captures all aspects of atomic electronic structure, and that a complete understanding of periodicity requires considering multiple complementary perspectives.

5.10. Statistical Correlation Validation

5.10.1. Wilks' Statistics Analysis

The Wilks' Lambda analysis revealed that the S, I, and D IT measures provide a natural representation of the periodicity of the elements. As illustrated in the previous 3D-plots, each period is clearly distinguishable within the Shannon–Fisher–disequilibrium space for both position and momentum representations. This observation is corroborated by Λ values lower than 0.1 in both spaces (see Table 2), indicating a statistically significant separation between elements grouped by period. Conversely, classifications based on blocks, group numbers and chemical families yielded Λ values close to one, indicating high group overlap.

Table 2. Λ values for the S, I, and D triads in position (r) and momentum (p) spaces for each of the common element classifications.

Classification	$\Lambda(r)$	$\Lambda(p)$
Periods	0.0732	0.0452
Blocks	0.637	0.647
Numeric Groups	0.844	0.795
Chemical Families	0.953	0.639

Notably, periodicity is particularly well-represented in momentum space. The lower Λ value obtained in this space is consistent with the visual evidence from the 3D plots (Figure 13), where periods appeared clearly separated in the momentum space triad.

5.10.2. Random Forest Analysis

The Random Forest results corroborate both the Wilks' statistical analysis and the visual evidence from the 3D plots. The highest predictive accuracy was achieved when predicting the elements' periods using IT triads in both position and momentum spaces (Table 3), indicating a strong correlation between the IT measures and periodicity. Conversely, accuracies for the other two classifications hovered around 33% (the expected baseline for random guessing), suggesting that the IT triads do not effectively encode these particular chemical classifications.

Table 3. Cross-validated accuracies of Random Forest models trained using the S, I, and D triads in position (r) and momentum (p) spaces to predict common element classifications.

Classification	Accuracy (%, r)	Accuracy (%, p)
Periods	78.7	69.0
Chemical Families	49.4	49.6
Blocks	48.6	56.1
Numeric Groups	24.2	28.0

In summary, both statistical analyses confirm the visual trends. These results validate the distinct separation of periods observed in the Shannon–Fisher–disequilibrium space for both position and momentum representations. Collectively, this constitutes formal evidence that these properties are intrinsically linked to the periodic nature of the elements, supporting the hypothesis that the helical-like shape is a natural representation of the periodic table in Shannon–Fisher–disequilibrium IT space.

6. Conclusions

This comprehensive information-theoretic analysis of atomic electron densities across the periodic table reveals that Shannon entropy, Fisher information, and disequilibrium provide a cohesive and rigorous structure of chemical periodicity. Within this three-dimensional information space—defined by Shannon entropy, Fisher's information system, and disequilibrium—the periodic table arises as a helicoidal progression, embedded in information space with a particular segmenting of periods across this global trajectory. It is important to emphasize that the helicoidal character is a genuine emergent property and is not imposed a priori.

There are a number of key findings in the analysis. First, Shannon entropy systematically decreases with atomic number, characteristic of progressive electronic localization; Fisher information and disequilibrium grow, representing increasing gradient content and density of electrons. The second conclusion is that the relationship between pairs of information-theoretic measures is universal, characterized by well marked global trends that are modulated by slight deviations at shell onsets. Third, there are chemical anomalies, like the exceptional configurations of Cr and Cu with distinct information-theoretic features that indicate the sensitivity of these measures to subtle electronic structure results. Fourth, the triadic analysis concerning halogens supports the geometric statement of hydrogen's double chemical nature as well as the unique nature of Period 1 elements. Most importantly, complexity measures (LMC and FS) display a monotonic increase with atomic number, providing a general characterization of atomic structural complexity across the periodic table. Fifth, the complementing analysis in momentum space results in broadest differentiation at low atomic number and the greatest compression for heavy substances, in the framework of uncertainty.

Perhaps one of the most relevant results of this work arises from the dual behavior of hydrogen: from the perspective of kinetic energy distribution and momentum-space electronic structure, hydrogen occupies a natural intermediate position between noble gases (low kinetic energy, tightly bound) and alkali metals (higher kinetic energy, more loosely bound). While position-space analysis emphasizes hydrogen's unique spatial delocalization, momentum-space analysis reveals that its characteristic kinetic energy places it between the kinetic extremes represented by He and Li. This result is potentially significant for ongoing discussions about optimal periodic table representations. Traditional position-space-based approaches suggest hydrogen's uniqueness and ambiguous placement. However, the momentum-space information-theoretic perspective suggests that hydrogen fits into a natural periodic sequence when kinetic energy structure is considered. This does not resolve the debate about hydrogen's optimal position, but it provides a new quantitative argument from a complementary perspective. Different representations (position-space vs. momentum-space, real-space vs. reciprocal-space) may be most appropriate for different chemical questions. Our findings provide quantitative data bearing on the hydrogen placement question, but we do not advocate for any specific resolution. The 3D IT representation of the elements in position space aligns with the view that *H* does not belong to either the alkali metals or the halogens, but rather stands as a unique, standalone element. This particular positioning of hydrogen in IT space is a mathematical

result that can inform, but does not resolve, the ongoing discussion among educators and philosophers of chemistry regarding optimal periodic table design.

The results of this study establish information theory as a quantitative and insightful approach to understanding atomic structure and chemical periodicity, providing an alternative perspective that complements traditional quantum mechanical descriptions while offering new insights into the fundamental organization of the elements. It is worth emphasizing that information-theoretic analysis provides objective, quantitative descriptors derived from quantum mechanical calculations without presupposing any particular periodic table format. As we demonstrate in the present work, the helicoidal structure emerges naturally from the IT measures; it is not an assumption of our methodology. In this sense, our results describe a mathematical structure inherent in atomic electronic organization.

On the other hand, we acknowledge that scalar relativistic and spin–orbit effects become significant for heavy elements ($Z > 50$), causing orbital contraction and expansion as well as fine-structure splitting. However, these effects modify quantitative properties while preserving the qualitative periodic structure. The organization into s, p, d, and f blocks remains intact, and as our results demonstrate, the information-theoretic helicoidal manifold persists throughout $Z = 1$–103. A comparative study using relativistic wave functions would be valuable future work.

Supplementary Materials: The following supporting information can be downloaded at: https://www.mdpi.com/article/10.3390/quantum8010022/s1, Video S1: Animated rotation of the 3D plot of the disequilibrium–Fisher–Shannon information-theoretic components in position space, for atomic elements $Z = 1$ through 103.

Author Contributions: Conceptualization, R.O.E.; methodology, R.O.E.; validation, R.O.E. and H.V.-H.; formal analysis, R.O.E., J.O.-M. and H.V.-H.; investigation, R.O.E. and H.V.-H.; writing—original draft preparation, R.O.E.; writing—review and editing, R.O.E. and H.V.-H.; visualization, R.O.E. All authors have read and agreed to the published version of the manuscript.

Funding: This research received no external funding.

Data Availability Statement: The raw data supporting the conclusions of this article will be made available by the authors on request.

Acknowledgments: R.O.E. whishes to thank Juan Carlos Angulo (University of Granada) for sharing his atomic data. Allocation of supercomputing resources are acknowledged from the Laboratorio de Supercómputo y Visualización at UAM. Also, H.V.-H. thanks for financial support from the Secretaría de Ciencia, Humanidades, Tecnología e Innovación (Secihti, México) for a PhD scholarship (CVU: 993929).

Conflicts of Interest: The authors declare no conflicts of interest.

References

1. Mendeleev, D.I. Sootnoshenie svoistv s atomnym vesom elementov. *Zhurnal Rus. Fiz.-Khimicheskogo Obs.* **1869**, *1*, 60–79.
2. Mendeleev, D.I. Estestvennaya sistema elementov i primenieee k ukazaniyu svoistv neotkrytykh elementov. *Zhurnal Rus. Fiz.-Khimicheskogo Obs.* **1871**, *3*, 25–56.
3. Van Spronsen, J.W. *The Periodic System of Chemical Elements: A History of the First Hundred Years*; Elsevier: Amsterdam, The Netherlands, 1969.
4. Scerri, E.R. *The Periodic Table: Its Story and Its Significance*; Oxford University Press: Oxford, UK, 2007.
5. Petruševski, V.M.; Cvetković, J. On the 'True Position' of Hydrogen in the Periodic Table. *Found. Chem.* **2018**, *20*, 251–260. [CrossRef]
6. Labarca, M.; Srivaths, A. On the Placement of Hydrogen and Helium in the Periodic System: A New Approach. *Chem. Bulg. J. Sci. Educ.* **2016**, *25*, 514–530.
7. Dash, H.H. Constant Energy Differences in Atomic Structure. *Nature* **1963**, *198*, 25–26. [CrossRef]
8. Dash, H.H. Position of Hydrogen in the Periodic System of Elements. *Nature* **1964**, *202*, 1001–1003. [CrossRef]

9. Sacks, L.J. Concerning the Position of Hydrogen in the Periodic Table. *Found. Chem.* **2006**, *8*, 31–35. [CrossRef]
10. Langmuir, I. The Arrangements of Electrons in Atoms and Molecules. *J. Am. Chem. Soc.* **1919**, *41*, 868–934. [CrossRef]
11. Luder, W.F. Electron Configuration as the Basis of the Periodic Table. *J. Chem. Educ.* **1943**, *20*, 21–26. [CrossRef]
12. Janet, C. *La Classification Hélicoïdale des Éléments Chimiques*; Imprimerie Deépartementale de L'Oise: Beauvais, France, 1928.
13. Janet, C. The Helicoidal Classification of the Elements. *Chem. News* **1929**, *138*, 372–374.
14. Katz, G. The Periodic Table: An Eight-Period Table for the 21st Century. *Chem. Educ.* **2001**, *6*, 324–332. [CrossRef]
15. Bohr, N. *The Theory of Spectra and Atomic Constitution*; The University Press: Cambridge, UK, 1922.
16. Scerri, E.R. Chemistry, Spectroscopy, and the Question of Reduction. *J. Chem. Educ.* **1991**, *68*, 122–126. [CrossRef]
17. Simmons, L.M. A Modification of the Periodic Table. *J. Chem. Educ.* **1947**, *24*, 588–591. [CrossRef]
18. Schwarz, W.H.E. The Full Story of Electron Configurations. *J. Chem. Educ.* **2010**, *87*, 444–448. [CrossRef]
19. Sanderson, R.T. A Rational Periodic Table. *J. Chem. Educ.* **1964**, *41*, 187–189. [CrossRef]
20. Allen, L.C. Electronegativity is the Average One-Electron Energy of the Valence-Shell Electrons in Ground-State Free Atoms. *J. Am. Chem. Soc.* **1989**, *111*, 9003–9014. [CrossRef]
21. Leach, M.R. Concerning Electronegativity as a Basic Elemental Property and Why the Periodic Table is Usually Represented in Its Medium Form. *Found. Chem.* **2013**, *15*, 13–29. [CrossRef]
22. Rayner-Canham, G.; Overton, T. *Descriptive Inorganic Chemistry*; Academic Press: Cambridge, MA, USA, 2010.
23. Scerri, E.R. The Role of Triads in the Evolution of the Periodic Table: Past and Present. *J. Chem. Educ.* **2008**, *85*, 585–589. [CrossRef]
24. Scerri, E.R. Explaining the Periodic Table, and the Role of Chemical Triads. *Found. Chem.* **2010**, *12*, 69–83. [CrossRef]
25. Bent, H.A. New Ideas in Chemistry from Fresh Energy for the Periodic Law. *J. Chem. Educ.* **2006**, *84*, 1431.
26. Firsching, F.H. Anomalies in the Periodic Table. *J. Chem. Educ.* **1981**, *58*, 478–479. [CrossRef]
27. Mendeleev, D.I. Die periodische Gesetzmässigkeit der chemischen Elemente. *Ann. Chem. Pharm.* **1870**, *8*, 133–229.
28. Stewart, P.J. A Century on from Dmitrii Mendeleev: Tables and Spirals, Noble Gases and Nobel Prizes. *Found. Chem.* **2007**, *9*, 235–245. [CrossRef]
29. Maeno, Y.; Hagino, K.; Ishiguro, T. Three related topics on the periodic tables of elements. *Found. Chem.* **2021**, *23*, 201–214. [CrossRef]
30. Leach, M. R. The Internet Database of Periodic Tables. 1999. Available online: https://www.meta-synthesis.com/webbook/35_pt/pt_database.php (accessed on 6 March 2026).
31. Kaesz, H.; Atkins, P.W. A Central Position for Hydrogen in the Periodic Table. *Chem. Int.* **2003**, *25*, 14. [CrossRef]
32. Rodríguez Peña, M.; García Guerra, J.A. The Periodic Spiral of Elements. *Found. Chem.* **2024**, *26*, 315–321. [CrossRef]
33. Imyanitov, N.S. Spiral as the Fundamental Graphic Representation of the Periodic Law. Blocks of Elements as the Autonomic Parts of the Periodic System. *Found. Chem.* **2016**, *18*, 153–173. [CrossRef]
34. Scherer, J.A. Models of a Spiral Periodic Chart. *J. Chem. Educ.* **1949**, *26*, 113–117. [CrossRef]
35. Stewart, P.J. Charles Janet: Unrecognized Genius of the Periodic System. *Found. Chem.* **2010**, *12*, 5–15. [CrossRef]
36. Janet, C. *Concordance de L'arrangement Quantique de Base des Électrons Planétaires des Atomes Avec la Classification Scalariforme, Hélicoïdale des Elements Chimiques*; Imprimerie Départementale de l'Oise: Beauvais, France, 1930.
37. Tsimmerman, V. Perfect Periodic Table. 2008. Available online: https://perfectperiodictable.com/ (accessed on 6 March 2026).
38. Kurushkin, M. Viatscheslaw Romanoff: Unknown Genius of the Periodic System. *Pure Appl. Chem.* **2019**, *91*, 1921–1928. [CrossRef]
39. Laing, M. Where to Put Hydrogen in a Periodic Table? *Found. Chem.* **2007**, *9*, 127–137. [CrossRef]
40. Rich, R.L. Are Some Elements More Equal Than Others? *J. Chem. Educ.* **2005**, *82*, 1761–1763. [CrossRef]
41. Scerri, E.R. Mendeleev's Periodic Table is Finally Completed and What to Do About Group 3. *Chem. Int.* **2012**, *34*, 28–31. [CrossRef]
42. Esquivel, R.O.; Angulo, J.C.; Antolín, J.; Dehesa, J.S.; López-Rosa, S.; Flores-Gallegos, N. Analysis of complexity measures and information planes of selected molecules in position and momentum spaces. *Phys. Chem. Chem. Phys.* **2010**, *12*, 7108. [CrossRef]
43. Esquivel, R.O.; López-Rosa, S.; Molina-Espíritu, M.; Angulo, J.C.; Dehesa, J.S. Information-theoretic space from simple atomic and molecular systems to biological and pharmacological molecules. *Theor. Chem. Acc.* **2016**, *135*, 253. [CrossRef]
44. Esquivel, R.O.; Flores-Gallegos, N.; Iuga, C.; Carrera, E.M.; Angulo, J.C.; Antolín, J. Phenomenological description of the transition state, and the bond breaking and bond forming processes of selected elementary chemical reactions: An information-theoretic study. *Theor. Chem. Acc.* **2009**, *124*, 445–460. [CrossRef]
45. López-Rosa, S.; Esquivel, R.O.; Angulo, J.C.; Antolín, J.; Dehesa, J.S.; Flores-Gallegos, N. Fisher Information Study in Position and Momentum Spaces for Elementary Chemical Reactions. *J. Chem. Theory Comput.* **2010**, *6*, 145–154. [CrossRef]
46. Vázquez-Hernández, H.; Esquivel, R.O. Phenomenological description of the acidity of the citric acid and its deprotonated species: Informational-theoretical study. *J. Mol. Model.* **2023**, *29*, 253. [CrossRef]

47. Esquivel, R.O.; Molina-Espíritu, M.; López-Rosa, S.; Soriano-Correa, C.; Barrientos-Salcedo, C.; Kohout, M.; Dehesa, J.S. Predominant Information Quality Scheme for the Essential Amino Acids: An Information-Theoretical Analysis. *ChemPhysChem* **2015**, *16*, 2571–2581. [CrossRef] [PubMed]
48. Vedral, V. *Introduction to Quantum Information Science*; Oxford University Press: New York, NY, USA, 2006.
49. Davidson, E.R. *Reduced Density Matrices in Quantum Chemistry*; Academic Press: Cambridge, MA, USA, 1976.
50. Koga, Y. Analytical Hartree-Fock electron densities for atoms He through Lr. *Theor. Chem. Acc.* **1997**, *95*, 113–130. [CrossRef]
51. Gubler, M.; Schäfer, M.R.; Behler, J.; Goedecker, S. Accuracy of charge densities in electronic structure calculations. *J. Chem. Phys.* **2025**, *162*, 094103. [CrossRef]
52. Hartree-Fock Method. Available online: https://www.sciencedirect.com/topics/chemistry/hartree-fock-method (accessed on 6 March 2026).
53. Angulo, J.C.; Antolín, J.; Esquivel, R.O. Atomic and molecular complexities: Their physical and chemical interpretations. In *Statistical Complexities: Applications in Electronic Structures*; Sen, K.D., Ed.; Springer: Berlin/Heidelberg, Germany, 2010.
54. Koga, T.; Kanayama, K.; Watanabe, S.; Thakkar, A.J. Analytical Hartree–Fock wave functions subject to cusp and asymptotic constraints: He to Xe, Li^+ to Cs^+, H^- to I^-. *Int. J. Quantum Chem.* **1999**, *71*, 491–497. [CrossRef]
55. Koga, T.; Kanayama, K.; Watanabe, S.; Imai, T.; Thakkar, A.J. Analytical Hartree–Fock wave functions for the atoms Cs to Lr. *Theor. Chem. Acc.* **2000**, *104*, 411–413. [CrossRef]
56. Rawlings, D.C.; Davidson, E.R. Molecular electron density distributions in position and momentum space. *J. Phys. Chem.* **1985**, *89*, 969–974. [CrossRef]
57. Kaijser, P.; Smith, V.H. Evaluation of Momentum Distributions and Compton Profiles for Atomic and Molecular Systems. In *Advances in Quantum Chemistry*; Elsevier: Amsterdam, The Netherlands, 1977; Volume 10, pp. 37–76. [CrossRef]
58. Baerends, E.J.; Aguirre, N.F.; Austin, N.D.; Autschbach, J.; Bickelhaupt, F.M.; Bulo, R.; Cappelli, C.; Van Duin, A.C.T.; Egidi, F.; Fonseca Guerra, C.; et al. The Amsterdam Modeling Suite. *J. Chem. Phys.* **2025**, *162*, 162501. [CrossRef]
59. Shannon, C.E. A Mathematical Theory of Communication. *Bell Syst. Tech. J.* **1948**, *27*, 379–423. [CrossRef]
60. Fisher, R.A. Theory of Statistical Estimation. *Math. Proc. Camb. Philos. Soc.* **1925**, *22*, 700–725. [CrossRef]
61. Frieden, B.R. *Science from Fisher Information: A Unification*; Cambridge University Press: Cambridge, UK, 2004.
62. Hamilton, I.P.; Mosna, R.A. Fisher information and kinetic energy functionals: A dequantization approach. *J. Comput. Appl. Math.* **2010**, *233*, 1542–1547. [CrossRef]
63. Onicescu, O. Théorie de l'information. Énergie informationnelle. *C. R. Acad. Sci. Paris Sér. A* **1966**, *263*, 841–842.
64. Carbo, R.; Leyda, L.; Arnau, M. How similar is a molecule to another? An electron density measure of similarity between two molecular structures. *Int. J. Quantum Chem.* **1980**, *17*, 1185–1189. [CrossRef]
65. López-Ruiz, R.; Mancini, H.; Calbet, X. A statistical measure of complexity. *Phys. Lett. A* **1995**, *209*, 321–326. [CrossRef]
66. Anteneodo, C.; Plastino, A. Some features of the López-Ruiz-Mancini-Calbet (LMC) statistical measure of complexity. *Phys. Lett. A* **1996**, *223*, 348–354. [CrossRef]
67. Romera, E.; Dehesa, J.S. The Fisher–Shannon information plane, an electron correlation tool. *J. Chem. Phys.* **2004**, *120*, 8906–8912. [CrossRef] [PubMed]
68. Sen, K. (Ed.) *Statistical Complexity: Applications in Electronic Structure*; Springer: Dordrecht, The Netherlands, 2011. [CrossRef]
69. Yamano, T. A statistical complexity measure with nonextensive entropy and quasi-multiplicativity. *J. Math. Phys.* **2004**, *45*, 1974–1987. [CrossRef]
70. Wilks, S.S. Certain generalizations in the analysis of variance. *Biometrika* **1932**, *24*, 471–494. [CrossRef]
71. Seabold, S.; Perktold, J. statsmodels: Econometric and statistical modeling with python. In Proceedings of the 9th Python in Science Conference, Austin, TX, USA, 28 June–3 July 2010.
72. Breiman, L. Random forests. *Mach. Learn.* **2001**, *45*, 5–32. [CrossRef]
73. Pedregosa, F.; Varoquaux, G.; Gramfort, A.; Michel, V.; Thirion, B.; Grisel, O.; Blondel, M.; Prettenhofer, P.; Weiss, R.; Dubourg, V.; et al. Scikit-learn: Machine Learning in Python. *J. Mach. Learn. Res.* **2011**, *12*, 2825–2830.